

The structure of fluctuations near mean-field critical points and spinodals and its implication for physical processes

W. Klein

*Department of Physics and Center for Computational Science,
Boston University, Boston, Massachusetts 02215, USA*

Harvey Gould

*Department of Physics, Clark University,
Worcester, Massachusetts 01610, USA*

Natali Gulbahce

*Theoretical Division and Center for Nonlinear Studies,
Los Alamos National Laboratory, Los Alamos, New Mexico 87545, USA**

J. B. Rundle

*Department of Physics and Center for Computational Science and Engineering,
University of California, Davis, California 95616, USA*

K. Tiampo

Earth Science Department, University of Western Ontario, London, Ontario N6A 5B7 Canada

We analyze the structure of fluctuations near critical points and spinodals in mean-field and near-mean-field systems. Unlike systems that are non-mean-field, for which a fluctuation can be represented by a single cluster in a properly chosen percolation model, the fluctuations in mean-field and near-mean-field systems consist of a large number of clusters that we refer to as fundamental clusters. The structure of the fundamental clusters and the way that they form fluctuations has important consequences for understanding phenomena as diverse as nucleation, spinodal decomposition and continuous ordering, and the statistical distribution of earthquakes. The effects related to the existence of fundamental clusters implies that these clusters are physical objects and not only mathematical constructs. These clusters and their effects are not easily describable by the standard methods of statistical mechanics.

I. INTRODUCTION

Systems that are mean-field or near-mean-field are common in nature. Examples of systems that can be classified as mean-field or near-mean-field include metals with long-range elastic forces [1, 2], earthquake faults with long-range stress transfer Green's functions [3], and polymers [4]. The connection between the range of the interaction and mean-field behavior was made by Kac and collaborators [5] who noted that a system with a pairwise additive potential of the form

$$V(x) = V_R(x) + \gamma^d \Phi(\gamma x), \quad (1)$$

becomes mean-field in the limit $\gamma \rightarrow 0$. In Eq. (1) $x = |\mathbf{x}|$ and $V_R(x)$ is a reference potential that is usually short range. The limit $\gamma \rightarrow 0$ is taken after the thermodynamic limit and before a critical point is approached. In addition, it is required that [5]

$$\int d\mathbf{x} \gamma^d |\Phi(\gamma x)| = A < \infty. \quad (2)$$

so that the energy per particle or spin remains finite in the $\gamma \rightarrow 0$ limit. The interaction range R is defined by the second moment of the potential,

$$R^2 \propto \int d\mathbf{x} x^2 \gamma^d \Phi(\gamma x) \propto \gamma^{-2}. \quad (3)$$

Hence, as $\gamma \rightarrow 0$, $R \rightarrow \infty$. We will refer to systems in which $R \gg 1$ but is not infinite as *near-mean-field*; systems with $R \rightarrow \infty$ are *mean-field* [6].

It has been shown in many studies that the kinetics of phase transitions is quite different in systems with $R \gg 1$ than in systems for which $R \sim 1$. Nucleation in near-mean-field systems often occurs near a pseudospinodal [7–9] where the surface tension is small, which in turn results in a nucleating droplet that has a very different structure [10–17] than that found in classical nucleation which occurs near the coexistence curve [18, 19].

The early stage growth of the peak of the equal time structure function during continuous ordering and spinodal decomposition in near-mean-field systems is described by the Cahn-Hilliard-Cook linear theory [20–22] for a time proportional to $\ln R$ after the quench [4]. In

*Formerly at Department of Physics, Clark University, Worcester, Massachusetts 01610, USA

addition, the morphology of the early stage evolution is quite different from that seen in systems with $R \sim 1$ [23–25].

In earthquake fault models it has been shown that in the mean-field limit the system can be described by an equilibrium theory [3, 26, 27]. In near-mean-field systems the smaller earthquake events are related to fluctuations about the pseudospinodal [3], and the very large (characteristic) events have a different character [28].

In these and other examples understanding the structure of the fluctuations near mean-field critical points and spinodals is important for understanding the behavior of the system. In this paper we analyze of the structure of the fluctuations and its relation to the underlying clusters and discuss the results of simulations done to test the theoretical predictions. We use field theory, scaling arguments, and cluster analysis to describe the fluctuation morphology and relate the structure to the nature of nucleation, the possible existence of a pseudospinodal in supercooled fluids, and the behavior of the driven diffusive models used to study earthquake faults.

In order that the paper be as self-contained as possible, we discuss in Secs. II, III, and V the standard ϕ^4 Landau-Ginzburg theory [29], the Parisi-Sourlas [30, 31] approach based on the Langevin equation with random Gaussian noise to study fluctuations near mean-field critical points, and the mapping of thermal systems onto properly chosen percolation models. In Sec. IV we use the same field theory techniques to discuss fluctuations near the spinodal and pseudospinodal. In Sec. VI we discuss the fluctuation morphology for mean-field and near-mean-field systems. In Sec. VII we return to the Landau-Ginzburg and Parisi-Sourlas approaches and discuss the relation of the fluctuations to the clusters. In Sec. VIII we examine the relation between the fluctuation structure and spinodals in supercooled fluids, and in Sec. IX we discuss the relation between the fluctuation structure and nucleation. In Sec. X we relate the cluster structure to earthquakes in associated cellular automaton models. Finally, in Sec. XI we summarize our results and discuss future work.

II. FIELD THEORY: LANDAU-GINZBURG

We will first discuss mean-field and near-mean-field systems from the perspective of field theory. The first approach is an equilibrium theory based on the work of Landau and Ginzburg [29]. The time-dependent approach is discussed in Sec. III and is based on the

work of Landau and Ginzburg [29] and Parisi and Sourlas [30, 31]. Both approaches begin with the Landau-Ginzburg free energy and the Landau-Ginzburg-Wilson Hamiltonian [32], which is taken to be [32, 33]

$$H(\phi) = \int d\mathbf{x} \left[\frac{R^2}{2} (\nabla \phi(\mathbf{x}))^2 + \epsilon \phi^2(\mathbf{x}) + \phi^4(\mathbf{x}) - h \phi(\mathbf{x}) \right]. \quad (4)$$

The range of interaction R arises from the second moment of the interaction between particles or spins through the gradient expansion. Without loss of generality we have set the proportionality constant in Eq. (3) equal to one. The partition function Z is

$$Z = \int \delta\phi e^{-\beta H(\phi(\mathbf{x}))}, \quad (5)$$

and the probability of a state $\phi(\mathbf{x})$ is

$$P(\phi) = \frac{e^{-\beta H(\phi)}}{Z}. \quad (6)$$

where $\beta = (k_B T)^{-1}$.

We are interested in mean-field or near-mean-field systems as described in Sec. I. To exploit this fact, we will scale all lengths with R . In this section we will concentrate on the critical point rather than the spinodal, which we will consider in Sec. IV. To study the critical point we set $h = 0$ and assume that

$$\epsilon = \frac{T - T_c}{T_c} \ll 1, \quad (7)$$

where T_c is the critical temperature. For $\epsilon \ll 1$ and $h = 0$ we can use scaling arguments. It is straightforward to see from Eq. (4) that

$$H(\tilde{\phi}) = R^d \epsilon^{2-d/2} \int d\mathbf{y} \left[\frac{1}{2} (\tilde{\nabla} \tilde{\phi}(\mathbf{y}))^2 + \tilde{\phi}^2(\mathbf{y}) + \tilde{\phi}^4(\mathbf{y}) \right], \quad (8)$$

where $\mathbf{y} = \mathbf{x}/R\epsilon^{-1/2}$, $\tilde{\phi}(\mathbf{x}) = \epsilon^{-1/2}\phi(\mathbf{x})$, and $\tilde{\nabla} = R\nabla$. The partition function integral in Eq. (5) can be done with saddle point techniques if $R^d \epsilon^{2-d/2} \gg 1$. We can give this requirement for the validity of using saddle point techniques a physical meaning by examining the Ginzburg criterion [29], which states that a system is mean-field if the mean square fluctuations in the order parameter are negligible compared to the square of the order parameter [33]. The order parameter in the Landau-Ginzburg-Wilson Hamiltonian of Eq. (4) is $\xi^d \phi(\mathbf{x})$, which is the magnetization in the Ising model or the density in a fluid. The notation in the literature is somewhat confusing. The quantity $\phi(\mathbf{x})$ is often referred to in the

literature as the order parameter, although as it is used in Eq. (4) it is an order parameter density. The order parameter is the integral of $\phi(\mathbf{x})$ over the volume of the system. In the following, we will also use $\phi(\mathbf{x})$ to designate objects, such as fluctuations in the order parameter density, that have a finite spatial extent. Although this dual use of $\phi(\mathbf{x})$ can be confusing, the meaning should be clear from the context.

The correlation length ξ is proportional to the linear spatial extent of the order parameter fluctuations. The mean square fluctuations in the order parameter are characterized by $\xi^d \chi_T$, where χ_T is the isothermal susceptibility [33]. In the vicinity of a mean-field critical point in the ϕ^4 model we have that [34]

$$\xi \sim R\epsilon^{-1/2} \quad (9a)$$

$$\phi \sim \epsilon^{1/2} \quad (9b)$$

$$\chi_T \sim \epsilon^{-1}. \quad (9c)$$

The Ginzburg criterion requires that

$$\frac{\xi^d \chi_T}{\xi^{2d} \phi^2} \rightarrow 0. \quad (10)$$

If we substitute the scaling forms in Eq. (9) into Eq. (10), we obtain

$$G = R^d \epsilon^{2-d/2} \rightarrow \infty. \quad (11)$$

We will refer to $G = R^d \epsilon^{2-d/2}$ as the Ginzburg parameter. In the limit $G \rightarrow \infty$ the system is mean-field. For $G \gg 1$ the system is near-mean-field.

The integral in Eq. (5) can be done exactly with a saddle point method if the system is mean-field. For near-mean-field systems, $G \gg 1$, and the saddle point approximation is reasonable. From these considerations we see that near critical points the criterion for mean-field and near-mean-field behavior is modified from the simple $R \rightarrow \infty$ for mean-field and $R \gg 1$ for near-mean-field discussed in Sec. I to similar criteria for G . Note that these criteria give the well known result that the upper critical dimension at the critical point in this system, above which the system has mean-field critical exponents for all R , including $R \sim 1$, is four [33].

From Eqs. (6) and (8) we have

$$P(\tilde{\phi}) = \frac{\exp \left\{ -\beta R^d \epsilon^{2-d/2} \int d\mathbf{y} \left[\frac{1}{2} (\tilde{\nabla} \tilde{\phi}(\mathbf{y}))^2 + \tilde{\phi}^2(\mathbf{y}) + \tilde{\phi}^4(\mathbf{y}) \right] \right\}}{Z}. \quad (12)$$

We will assume for the moment that for $G = R^d \epsilon^{2-d/2} \gg 1$, the Landau-Ginzburg-Wilson Hamiltonian can be well approximated by a Gaussian [33]. We have

$$P_G(\tilde{\phi}) = \frac{\exp \left\{ -\beta R^d \epsilon^{2-d/2} \int d\mathbf{y} [\frac{1}{2}(\tilde{\nabla} \tilde{\phi}(\mathbf{y})]^2 + \tilde{\phi}^2(\mathbf{y})] \right\}}{Z_G}, \quad (13)$$

where Z_G is the functional integral over $\tilde{\phi}$ of the numerator in Eq. (13). We use $P_G(\tilde{\phi})$ to calculate the structure function $S(\tilde{k})$.

$$S(\tilde{k}) = \epsilon \langle \tilde{\phi}(\tilde{\mathbf{k}}) \tilde{\phi}(-\tilde{\mathbf{k}}) \rangle = \frac{\epsilon \int \delta \tilde{\phi}(\tilde{\mathbf{k}}) \exp[-\beta R^d \epsilon^{2-d/2} \int d\tilde{\mathbf{k}} (\tilde{k}^2 + 1) \tilde{\phi}(\tilde{\mathbf{k}}) \tilde{\phi}(-\tilde{\mathbf{k}})] \tilde{\phi}(\tilde{\mathbf{k}}) \tilde{\phi}(-\tilde{\mathbf{k}})}{Z_G}, \quad (14)$$

where $\tilde{\mathbf{k}} = R\epsilon^{-1/2}\mathbf{k}$ and $\tilde{\phi}(\mathbf{k}) = \tilde{\phi}(-\mathbf{k})$. Note that for $\epsilon > 0$ and $h = 0$, $\langle \tilde{\phi}(\mathbf{x}) \rangle = 0$. We have (in scaled variables)

$$S(\tilde{k}) \propto \frac{\epsilon}{R^d \epsilon^{2-d/2}} \frac{1}{\tilde{k}^2 + 1}. \quad (15)$$

The Fourier transform of Eq. (15) gives the pair distribution function, which we have written in terms of unscaled variables:

$$\rho^{(2)}(x) \sim \frac{1}{x^{d-2}} \frac{\epsilon}{R^d \epsilon^{2-d/2}} e^{-x/R\epsilon^{-1/2}}. \quad (16)$$

The $1/x^{d-2}$ dependence in Eq. (16) is valid for $d \geq 3$. For $d = 2$ this dependence is replaced by $1/x^{1/2}$; in $d = 1$, there is no x -dependence in the denominator. The form of the right-hand side of Eq. (16) implies that $R\epsilon^{-1/2}$ is the correlation length (see Eq. (9a)).

For scaling purposes we can treat $\rho^{(2)}(x)$ for $x \ll R\epsilon^{-1/2}$ as a constant. Hence $\rho^{(2)}$ for $x \ll R\epsilon^{-1/2}$ is proportional to the square of the density of a fluctuation and the fluctuations in the order parameter density scale as

$$\phi(\mathbf{x} \ll \xi) \sim \frac{\epsilon^{1/2}}{(R^d \epsilon^{2-d/2})^{1/2}} = \frac{\epsilon^{1/2}}{G^{1/2}}. \quad (17)$$

We see that the density of a critical phenomena fluctuation does not scale as $\epsilon^{1/2}$ as might be expected from a simple extension of how the global order parameter scales for $\epsilon < 0$ (see Eq. (9b)) [34] and in comparison with the Ising model with nearest-neighbor interactions in $d < 4$. Below the critical point the order parameter, in contrast to the fluctuations, does scale as $|\epsilon|^{1/2}$ as can be seen from Eq. (8) using $H(\phi)$ as a free energy. We will discuss this point more fully in Sec. IV. Note that the linear dimension of the fluctuations is the correlation length as it is in systems that are not mean-field. The scaling of $\phi(\mathbf{x})$ with $G^{-1/2}$

in Eq. (17) justifies neglecting the ϕ^4 term in Eq. (12) to obtain the Gaussian approximation in Eq. (13).

The pair distribution function $\rho^{(2)}$ in Eq. (16) satisfies the relation [33, 34]

$$\chi_T \propto \int d\mathbf{x} \rho^{(2)}(\mathbf{x}). \quad (18)$$

If we use the scaling form of $\phi(\mathbf{x})$ in Eq. (18), we find that $\chi_T \sim \epsilon^{-1}$, further evidence that the scaling of the order parameter density in Eq. (18) is correct.

We next discuss the Landau-Ginzburg and Cahn-Hilliard equations in mean-field and near-mean-field systems. One way to obtain these equations is to note that the time rate of change of an order parameter such as the density is related to the chemical potential μ . If the order parameter is not conserved and there are no other conservation laws (model A in the Hohenberg-Halperin classification scheme [35]), then

$$\frac{\partial \phi(t)}{\partial t} \propto -\mu \text{ and } \mu \propto \frac{\delta F(\phi)}{\delta \phi}, \quad (19)$$

where $F(\phi)$ is the free energy. We take $F(\phi)$ to be equal to the Landau-Ginzburg-Wilson Hamiltonian in Eq. (4), which is correct for mean-field systems and a good approximation in near-mean-field systems, and assume that the relations in Eq. (19) are valid in a spatial and time dependent context and when the derivatives are with respect to the function $\phi(\mathbf{x}, t)$. In this way we obtain the Landau-Ginzburg equation [19, 29]:

$$\frac{\partial \phi(\mathbf{x}, t)}{\partial t} = -M_A[-R^2 \nabla^2 \phi(\mathbf{x}, t) + 2\epsilon\phi(\mathbf{x}, t) + 4\phi^3(\mathbf{x}, t) - h] + \eta(\mathbf{x}, t), \quad (20)$$

where we have added a noise term $\eta(\mathbf{x}, t)$. For a conserved order parameter (model B in the Hohenberg-Halperin classification [35]) we have

$$\frac{\partial \phi(\mathbf{x}, t)}{\partial t} \propto \nabla \cdot \mathbf{J} \text{ and } \mathbf{J} \propto \nabla \mu(\mathbf{x}, t). \quad (21)$$

If we again use the Landau-Ginzburg-Wilson Hamiltonian in Eq. (4) as a free energy, we obtain the Cahn-Hilliard-Cook equation [19]

$$\frac{\partial \phi(\mathbf{x}, t)}{\partial t} = M_B \nabla^2 [-R^2 \nabla^2 \phi(\mathbf{x}, t) + 2\epsilon\phi(\mathbf{x}, t) + 4\phi^3(\mathbf{x}, t) - h] + \eta_c(\mathbf{x}, t), \quad (22)$$

where we have again added a noise term. The quantities M_A and M_B in Eqs. (20) and (22) are the mobilities. We will return to a discussion of the mobilities in Sec. III.

To obtain Eqs. (19) and (21) we need to assume local equilibrium. That is, we assume that within the coarse grained volume used to obtain the Landau-Ginzburg free energy [19], the system comes into equilibrium on a time scale short compared to the time scales of interest.

For the remainder of this paper we will take $\eta(\mathbf{x}, t)$ and $\eta_c(\mathbf{x}, t)$ to be random and Gaussian with a zero mean. That is

$$\langle \eta(\mathbf{x}, t) \rangle = \langle \eta_c(\mathbf{x}, t) \rangle = 0, \quad (23a)$$

$$\langle \eta(\mathbf{x}, t) \eta(\mathbf{x}', t') \rangle = k_B T \delta(\mathbf{x} - \mathbf{x}') \delta(t - t') \quad (23b)$$

$$\langle \eta_c(\mathbf{x}, t) \eta_c(\mathbf{x}', t') \rangle = k_B T \nabla^2 \delta(\mathbf{x} - \mathbf{x}') \delta(t - t') \quad (23c)$$

where T is the temperature and k_B is Boltzmann's constant.

We can now use Eqs. (20) and (22) to look at the time dependence of the decay of fluctuations in mean-field and near-mean-field systems. Because $G \gg 1$ in these systems, the scaling of the order parameter density $\phi(\mathbf{x})$ in Eq. (17) implies that the cubic term in Eqs. (20) and (21) can be neglected. A straightforward calculation shows that the fluctuations decay exponentially in both model A and model B with characteristic times that diverge as ϵ^{-1} in model A [33] and $R^2 \epsilon^{-2}$ in model B [33]. These points will be revisited in Sec. III. For the remainder of this paper we will consider only the time-dependence of model A given in Eq. (20).

III. FIELD THEORY: PARISI-SOURLAS

Another approach that is quite useful was introduced by Parisi and Sourlas [30, 31]. It begins with the Landau-Ginzburg equation (20) discussed in Sec. II. Because the noise $\eta(\mathbf{x}, t)$ in Eq. (20) is random Gaussian, the measure of the noise is [30, 31]

$$P(\eta) = \frac{\exp[-\beta \int d\mathbf{x} dt \eta^2(\mathbf{x}, t)]}{\int \delta\eta \exp[-\beta \int d\mathbf{x} dt \eta^2(\mathbf{x}, t)]}. \quad (24)$$

We now use Eq. (20) to replace $\eta(\mathbf{x}, t)$ in Eq. (24). For the purpose of this discussion we will restrict ourselves to $h = 0$. We obtain

$$\bar{P}(\phi) \propto J(\phi, \eta) \exp \left\{ -\beta \int d\mathbf{x} dt \left[\frac{\partial \phi(\vec{x}, t)}{\partial t} + M_A (-R^2 \nabla^2 \phi(\vec{x}, t) + 2\epsilon \phi(\vec{x}, t) + 4\phi^3(\vec{x}, t)) \right]^2 \right\}, \quad (25)$$

where $J(\phi, \eta)$, the Jacobian of the transformation from η to ϕ , is the determinant of the operator $\delta\eta(\mathbf{x}, t)/\delta\phi(\mathbf{x}, t)$. Following Parisi and Sourlas [30, 31] we introduce the Grassman variables $\psi_F(\mathbf{x}, t)$ and $\bar{\psi}_F(\mathbf{x}, t)$ which satisfy the algebra

$$\psi_F^2(\mathbf{x}, t) = \bar{\psi}_F^2(\mathbf{x}, t) = \int d\psi_F(\mathbf{x}, t) = \int d\bar{\psi}_F(\mathbf{x}, t) = 0, \quad (26)$$

$$\{\bar{\psi}_F(\mathbf{x}, t)\psi_F(\mathbf{x}, t) + \psi_F(\mathbf{x}, t)\bar{\psi}_F(\mathbf{x}, t)\} = 0, \quad (27)$$

$$\int \psi_F(\mathbf{x}, t)d\psi_F(\mathbf{x}, t) = \int \bar{\psi}_F(\mathbf{x}, t)d\bar{\psi}_F(\mathbf{x}, t) = 1. \quad (28)$$

Equation (27) implies that the variables anticommute. Parisi and Sourlas refer to $\psi_F(\mathbf{x}, t)$ and $\bar{\psi}_F(\mathbf{x}, t)$ as fermions and $\phi(\mathbf{x}, t)$ as a boson. With this algebra it is relatively easy to evaluate the Jacobian in Eq. (25) and write $\bar{P}(\phi)$ as

$$\bar{P}(\phi, \psi_F, \bar{\psi}_F) = \frac{\exp \left\{ -\beta \left[\int d\mathbf{x} dt (S_B(\phi, \psi_F, \bar{\psi}_F) + S_F(\phi, \psi_F, \bar{\psi}_F)) \right] \right\}}{\bar{Z}}, \quad (29)$$

where \bar{Z} is a normalization factor. The quantities S_B and S_F are given by

$$S_B(\phi, \psi_F, \bar{\psi}_F) = \int d\mathbf{x} dt \left[\frac{\partial \phi(\mathbf{x}, t)}{\partial t} + M_A (-R^2 \nabla^2 \phi(\mathbf{x}, t) + 2\epsilon \phi(\mathbf{x}, t) + 4\phi^3(\mathbf{x}, t)) \right]^2 \quad (30)$$

$$S_F(\phi, \psi_F, \bar{\psi}_F) = \int d\mathbf{x} dt \bar{\psi}_F(\mathbf{x}, t) \left[\frac{\partial}{\partial t} + M_A (-R^2 \nabla^2 + 2\epsilon + 12\phi^2(\mathbf{x}, t)) \right] \psi_F(\mathbf{x}, t). \quad (31)$$

We first focus on the term $S_B(\phi, \psi_F, \bar{\psi}_F)$. Among the terms produced by squaring the integrand is a term of the form

$$C(\phi) = 2M_A \int d\mathbf{x} dt \frac{\partial \phi(\mathbf{x}, t)}{\partial t} \left[-R^2 \nabla^2 \phi(\mathbf{x}, t) + 2\epsilon \phi(\mathbf{x}, t) + 4\phi^3(\mathbf{x}, t) \right], \quad (32)$$

which is equal to

$$2M_A \int d\mathbf{x} \int_{t_I}^{t_F} dt \frac{\partial}{\partial t} H(\phi), \quad (33)$$

where $H(\phi)$ is given by Eq. (4) with $h = 0$. We can do the integral with respect to t and obtain

$$C(\phi) = 2M_A \int d\mathbf{x} [H(\phi(\mathbf{x}, t_F)) - H(\phi(\mathbf{x}, t_I))]. \quad (34)$$

Parisi and Sourlas assume that t_F and t_I can be found such that $C(\phi) = 0$ and show that with this assumption there is a transformation that maps fermions and bosons into each other and keeps $\bar{P}(\phi)$ in Eq. (29) invariant. They refer to such systems as supersymmetric. If a system is in equilibrium, such values of t_I and t_F can always be found [30, 31].

For the purpose of investigating the morphology of fluctuations in the neighborhood of mean-field and near-mean-field critical points, the supersymmetric form of $\bar{P}(\phi, \psi_F, \bar{\psi}_F)$ is the proper representation. In mean-field or near-mean-field the Landau-Ginzburg-Wilson Hamiltonian in Eq. (4) can be assumed to be Gaussian as discussed in Sec. I. This assumption in turn implies that the Landau-Ginzburg and Cahn-Hilliard equations can be linearized for $G \gg 1$. Because the ϕ dependence in the fermionic part of the action $S_F(\phi, \psi_F, \bar{\psi}_F)$ comes from the nonlinear term in the Landau-Ginzburg equation, linearization of the Landau-Ginzburg equation makes the two parts of the action, $S_B(\phi, \psi_F, \bar{\psi}_F)$ and $S_F(\phi, \psi_F, \bar{\psi}_F)$, independent. The integration over the fermionic variables $\psi_F(\mathbf{x}, t)$ and $\bar{\psi}_F(\mathbf{x}, t)$ can be done immediately resulting in the measure

$$\bar{P}(\phi) = \frac{\exp \left\{ -\beta \int d\mathbf{x} dt \left(\frac{\partial \phi(\mathbf{x}, t)}{\partial t} \right)^2 + M_A^2 [-R^2 \nabla^2 \phi(\mathbf{x}, t) + \epsilon \phi(\mathbf{x}, t)]^2 \right\}}{Z_S}, \quad (35)$$

where the normalization constant Z_S is the functional integral over ϕ of the numerator in Eq. (35).

In equilibrium $\bar{P}(\phi)$ should give the same probability of a fluctuation as $P(\phi)$ in Eq. (6). To understand the relation between these two probabilities we note that if $P(\phi)$ is of order ϵ^{-1} , then $\bar{P}(\phi)$ should also be of order ϵ^{-1} . If we take ϕ to describe an equilibrium fluctuation from Eq. (35), we expect that

$$\int d\mathbf{x} dt \left(\frac{\partial \phi(\mathbf{x}, t)}{\partial t} \right)^2 \sim 1. \quad (36)$$

From the discussion in Sec. II we know that ϕ has a spatial extent that scales as the correlation length ξ so that from simple scaling arguments $d\mathbf{x}$ in Eq. (36) scales as $\xi^d \sim R^d \epsilon^{-d/2}$. We also know from Eq. (17) that $\phi(\mathbf{x}) \sim \epsilon^{1/2} / (R^d \epsilon^{2-d/2})^{1/2}$. We use these scaling relations and $dt/(dt)^2 \sim 1/\tau$ in Eq. (36) to obtain

$$\frac{(\epsilon^{1/2})^2 R^d \epsilon^{-d/2}}{\tau_{f,c} R^d \epsilon^{2-d/2}} \sim 1, \quad (37)$$

or

$$\tau_{f,c} \sim \epsilon^{-1}. \quad (\text{mean lifetime of fluctuations near mean-field critical point}) \quad (38)$$

Equation (38) is the well known scaling relation for critical slowing down near mean-field critical points for model A (see Sec. II) [35]. If we require that

$$\int d\mathbf{x} dt M_A^2 [-R^2 \nabla^2 \phi(\mathbf{x}, t) + \epsilon \phi(\mathbf{x}, t)]^2 \sim 1, \quad (39)$$

and use the scaling relations for ξ , ϕ , and $\tau_{f,c}$ and the same arguments used to obtain Eq. (37), we find

$$\frac{M_A^2 \epsilon^3 R^d \epsilon^{-d/2} \epsilon^{-1}}{R^d \epsilon^{2-d/2}} \sim 1, \quad (40)$$

or M_A is a constant of order 1.

These results are all expected. Note that there is a significant conceptual difference between $P(\phi)$ and $\bar{P}(\phi)$. The quantity $P(\phi)$ is the fraction of independent members of an ensemble in which $\phi(\mathbf{x})$ is realized when a measurement is made. Because the system is assumed to be in equilibrium, we can divide a time sequence of measurements into independent segments that can be thought of as members of an ensemble. These segments have a duration of the order of the decorrelation time (or longer) [36], which is of order $\tau_{f,c}$ near the critical point [35]. The quantity $\bar{P}(\phi)$ gives the probability of a “path” in ϕ space. The paths of interest for the purpose of this discussion are those whose probability is the order of ϵ^{-1} . As we have seen, the path that results in an object with an order parameter density (or $\phi(\mathbf{x})$) change of order $\epsilon^{1/2}/(R^d \epsilon^{2-d/2})^{1/2}$, linear dimension of order $\xi = R\epsilon^{-1/2}$, and a lifetime of order ϵ^{-1} is one such path.

Suppose that in equilibrium there is an object with a linear size of $\xi = R\epsilon^{-1/2}$ but a different density. In particular, suppose there is an object of density of $\phi_{fc} \sim \epsilon^{1/2}/R^d \epsilon^{2-d/2}$. We consider this density because it will later be seen to be relevant. Because we have assumed equilibrium, we have supersymmetry, and the action is the sum of two terms as in Eq. (35). One term has the the form as Eq. (36):

$$S_{B,1} = \int d\mathbf{x} dt \left(\frac{\partial \phi(\mathbf{x}, t)}{\partial t} \right)^2. \quad (41)$$

As with the fluctuations we define the lifetime of this object to be when $S_{B,1} \sim 1$. That is, we take the lifetime of an object $\tau_{fc,c}$ to be when $\bar{P}(\phi(\tau_{fc,c})) \sim \epsilon^{-1}$. We use the scaling forms for $\phi(\mathbf{x})$ and dx in Eq. (41) and obtain

$$\frac{\epsilon R^d \epsilon^{-d/2}}{\tau_{fc,c} (R^d \epsilon^{2-d/2})^2} \sim 1, \quad (42)$$

or

$$\tau_{fc,c} \sim \frac{\epsilon^{-1}}{R^d \epsilon^{2-d/2}} = \frac{\epsilon^{-1}}{G}. \quad (43)$$

Equation (43) gives the lifetime of an object with density $\phi_{fc} \sim \epsilon^{1/2}/R^d \epsilon^{2-d/2}$ near a mean-field critical point.

The Boltzmann probability of finding such an object $P(\phi)$ is

$$P(\phi) \propto \exp \left\{ -\beta \int d\mathbf{x} \left[\frac{R^2}{2} (\nabla \phi(\mathbf{x}))^2 + \epsilon \phi^2(\mathbf{x}) \right] \right\}. \quad (44)$$

If we use the scaling relations and set $\beta = 1$ for convenience, we obtain

$$P(\phi) \propto e^{-1/R^d \epsilon^{2-d/2}}. \quad (45)$$

We see that $P(\phi) \neq \bar{P}(\phi)$ in this case despite the fact that the system is in equilibrium. If we want the probability $\bar{P}(\phi)$ that there is a path that consists of an object with density $\phi_{fc} \sim \epsilon^{1/2}/R^d \epsilon^{2-d/2}$, linear dimension $\xi \sim R\epsilon^{-1/2}$, and duration ϵ^{-1} rather than $\epsilon^{-1}/R^d \epsilon^{2-d/2}$, then

$$\bar{P}(\phi) = P(\phi) \sim e^{-1/R^d \epsilon^{2-d/2}}, \quad (46)$$

and $P(\phi) = \bar{P}(\phi)$. The implication of these results is that the Boltzmann probability $P(\phi)$ requires a given time, that is, the decorrelation time, which near the mean-field critical point scales as ϵ^{-1} . The probability $\bar{P}(\phi)$ will equal $P(\phi)$ only if t is chosen to be the decorrelation time $\tau_{f,c}$. However, in general, the decorrelation time is not equal to the lifetime of the object of interest.

The mobility M_A need not be a constant independent of ϵ [19]. For an object with density $\phi_{fc} \sim \epsilon^{1/2}/R^d \epsilon^{2-d/2}$, the second term in the action in Eq. (25) has the form

$$S_2 = - \int d\mathbf{x} dt M_A^2 [R^2 (\nabla \phi(\mathbf{x}, t))^2 + 2\epsilon \phi(\mathbf{x}, t)]^2. \quad (47)$$

By using the scaling relations with the lifetime given by Eq. (43), we obtain

$$\frac{M_A^2 \epsilon^3 R^d \epsilon^{-d/2} \epsilon^{-1}}{(R^d \epsilon^{2-d/2})^3} \sim 1, \quad (48)$$

or

$$M_A \sim R^d \epsilon^{2-d/2} \gg 1. \quad (49)$$

Note that M_A in Eq. (49) depends on ϵ in contrast to the mobility given by Eq. (40). If we had considered a lifetime of ϵ^{-1} rather than the lifetime ϵ^{-1}/G in Eq. (43), M_A would be order unity.

In summary, the probabilities $P(\phi)$ and $\bar{P}(\phi)$ are equal if the lifetime of an object is the order of ϵ^{-1} near the mean-field critical point. The lifetime of an object is obtained by requiring that $\bar{P}(\phi) \sim e^{-1}$. This requirement follows from the fact that we expect

equilibrium objects to decay exponentially. Note that if there are objects with a density $\epsilon^{1/2}/G$ with a lifetime of ϵ^{-1}/G , the usual Boltzmann factor will not give the probability of observing such an object.

IV. SPINODALS AND PSEUDOSPINODALS

In this section we introduce the meaning of the spinodal and the pseudospinodal. We begin with the Landau-Ginzburg-Wilson Hamiltonian in Eq. (4). The partition function is given in Eq. (5). For $R \gg 1$ and $\epsilon > 0$ such that $G \gg 1$, the partition function can be evaluated using saddle point techniques. We will return to this point shortly. Hence, the free energy in the $G \rightarrow \infty$ limit is of the Landau-Ginzburg form [29],

$$F = \int d\mathbf{x} \left[\frac{R^2}{2} (\nabla\phi(\mathbf{x}))^2 + \epsilon\phi^2(\mathbf{x}) + \phi^4(\mathbf{x}) - h\phi(\mathbf{x}) \right]. \quad (50)$$

We set the gradient term equal to zero to obtain the free energy density

$$f = \epsilon\phi^2 + \phi^4 - h\phi. \quad (51)$$

For $\epsilon > 0$ there is only one real extremum of the free energy. For $\epsilon < 0$ there are three real extrema, one maximum and two minima. For $h = 0$ the two minima are the same depth, that is, there are two states with the same free energy. As the magnitude of h is increased, one of the minima becomes higher than the other. The higher minimum corresponds to the metastable state. Increasing $|h|$ further eventually results in the disappearance of the metastable minimum. This value of $|h|$ is referred to as the spinodal field h_s . It is simple to see from Eq. (51) that at $h = h_s$, f has an inflection point at a value of ϕ that we will call ϕ_s . If we set $\partial f / \partial \phi = \partial^2 f / \partial \phi^2 = 0$, we find

$$\phi_s = (|\epsilon|/6)^{1/2} \text{ and } h_s = 4|\epsilon|^{3/2}/(3\sqrt{6}). \quad (52)$$

We define a new variable Δh ,

$$\Delta h = h_s - h, \quad (53)$$

and a new field, $\phi(\mathbf{x}) - \phi_s$, and write the mean-field free energy as

$$F = \int d\mathbf{x} \left[\frac{R^2}{2} (\nabla\psi(\mathbf{x}))^2 + \Delta h^{1/2} \lambda_1 \psi^2(\mathbf{x}) - \lambda_2 \psi^3(\mathbf{x}) + \lambda_3 \psi^4(\mathbf{x}) \right], \quad (54)$$

where $\psi(\mathbf{x}) = \phi(\mathbf{x}) - \phi_s + a$; a is chosen so that the term linear in $\psi(\mathbf{x})$ does not appear in F . The coefficients λ_i are functions of ϵ , which we will always take to be nonzero, but are not functions of Δh . The free energy in Eq. (54) is constructed so that the spinodal is at $\psi = 0$ and $\Delta h = 0$.

As with the critical point we can assume that the fluctuations associated with the spinodal critical point can be described by a Gaussian Landau-Ginzburg-Wilson Hamiltonian with a partition function given by

$$Z = \int \delta\psi \exp \left[-\beta \int d\mathbf{x} \frac{R^2}{2} (\nabla\psi(\mathbf{x}))^2 + \Delta h^{1/2} \lambda_1 \psi^2(\mathbf{x}) \right]. \quad (55)$$

Following the same argument that we used at the critical point in Sec. II, we can show that

$$\xi \sim R\Delta h^{-1/4} \quad (56a)$$

$$\chi_T \sim \Delta h^{-1/2}. \quad (56b)$$

The fluctuation density scales near the spinodal as

$$\psi(\mathbf{x} \ll \xi) \sim \frac{\Delta h^{1/2}}{[R^d \Delta h^{3/2-d/4}]^{1/2}} = \frac{\Delta h^{1/2}}{G_s}, \quad (56c)$$

and the Ginzburg parameter near the spinodal is

$$G_s = R^d \Delta h^{3/2-d/4}. \quad (57)$$

As at the critical point, the system is mean-field when $G_s \rightarrow \infty$ and near-mean-field for $G_s \gg 1$. Spinodals are only true critical points in the mean-field limit [7–9].

As discussed in Sec. II the scaling of the order parameter density and the scaling of the fluctuations are not the same in mean-field and near-mean-field systems. The scaling of the order parameter density does not involve the Ginzburg parameter. For example, near the critical point for $\epsilon < 0$ we have from Eq. (51)

$$-2|\epsilon|\phi + 4\phi^3 = 0. \quad (58)$$

Equation (58) gives the order parameter density at the minima for $\epsilon < 0$. As $|\epsilon| \rightarrow 0$ we have

$$\phi \sim |\epsilon|^{1/2}. \quad (59)$$

Near the spinodal we use Eq. (54) and assume that $\psi(\mathbf{x})$ is independent of \mathbf{x} . We have

$$f(\psi) = \Delta h^{1/2} \lambda_1 \psi^2 - \lambda_2 \psi^3 + \lambda_3 \psi^4. \quad (60)$$

As $\Delta h \rightarrow 0$, ψ scales as

$$\psi \sim \Delta h^{1/2}, \quad (\text{scaling of order parameter density near spinodal}) \quad (61)$$

where we have dropped the ψ^4 term in Eq. (60). Equation (61) gives the scaling of the order parameter density, not the scaling of a fluctuation. As near the critical point, the scaling of the order parameter density and the fluctuations is not the same in mean-field or near-mean-field systems near the spinodal and pseudospinodal.

In the above discussion we kept the temperature fixed and approached the spinodal by varying the magnetic field h . Alternatively, we can keep the magnetic field fixed and approach the spinodal by varying the temperature. To obtain the critical exponents in the temperature variable we return to Eq. (51) and write ϵ as

$$\epsilon = \frac{T - T_c}{T_c} = \frac{T - T_s}{T_c} + \frac{T_s - T_c}{T_c} = \Delta\epsilon + \epsilon_s, \quad (62)$$

where T_s is the spinodal temperature for a fixed field $h = h_s$. We write

$$\left. \frac{\partial^2 f}{\partial \phi^2} \right|_{\phi=\phi_s} = -2|\Delta\epsilon| - 2|\epsilon|_s + 12\phi_s^2 + 24\phi_s\psi = 0, \quad (63)$$

Because ϵ_s and ϕ_s are on the spinodal curve, we have

$$-2|\epsilon_s| + 12\phi_s^2 = 0, \quad (64)$$

and

$$-2|\Delta\epsilon| + 24\phi_s\psi = 0. \quad (65)$$

From Eqs. (61) and (65) we have

$$\Delta h^{1/2} \sim \Delta\epsilon, \quad (66)$$

which implies from Eq. (56c) that as the spinodal is approached, the density of the fluctuations scales as

$$\psi(\mathbf{x}) \sim \frac{\Delta\epsilon}{[R^d \Delta\epsilon^{3-d/2}]^{1/2}} = \frac{\Delta\epsilon}{G_s^{1/2}}. \quad (67a)$$

The correlation length scales as

$$\xi \sim R\Delta\epsilon^{-1/2}, \quad (67b)$$

and the susceptibility diverges as

$$\chi_T \sim \Delta\epsilon^{-1}. \quad (67c)$$

Equations (67) and (56) give the critical exponents near the spinodal in terms of Δh and $\Delta\epsilon$, respectively.

Before we discuss the pseudospinodal, we discuss the application of the Parisi-Sourlas method in the neighborhood of the spinodal. If we construct a Landau-Ginzburg equation from the free energy in Eq. (54), we have

$$\frac{\partial\psi(\mathbf{x},t)}{\partial t} = -M_A \left[-R^2 \nabla^2 \psi(\mathbf{x},t) + 2\Delta h^{1/2} \lambda_1 \psi(\mathbf{x},t) - 3\lambda_2 \psi^2(\mathbf{x},t) + 4\lambda_3 \psi^3(\mathbf{x},t) \right] + \eta(\mathbf{x},t). \quad (68)$$

If we assume that the noise $\eta(\mathbf{x},t)$ is a random Gaussian, we obtain an expression for the probability of a path $\psi(\mathbf{x},t)$ of the form

$$\bar{P}_{\text{sp}}(\psi) = \frac{\exp \left[-\beta \int d\mathbf{x} dt \left(\frac{\partial\psi(\mathbf{x},t)}{\partial t} \right)^2 + M_A^2 \left\{ -R^2 \nabla^2 \psi(\mathbf{x},t) + 2\lambda_1 \Delta h^{1/2} \psi(\mathbf{x},t) \right\}^2 \right]}{Z_{\text{sp}}}, \quad (69)$$

where we have used only the linear form of the Landau-Ginzburg equation and have assumed that the system is in metastable equilibrium, which implies supersymmetry as in Sec. III. From arguments almost identical to those used at the critical point, we find that the relaxation or decorrelation time scales as

$$\tau \sim \Delta h^{-1/2}. \quad (\text{decorrelation time near the spinodal}) \quad (70)$$

All considerations of the difference between Boltzmann factors and probabilities of paths are the same near spinodals and critical points.

We now turn to a discussion of the pseudospinodal. As mentioned, the spinodal is a mean-field object. For $G_s \gg 1$ but finite, there is no spinodal. However, the system behaves as if it existed if G_s is sufficiently large. In Fig. 1 we plot the inverse of the isothermal susceptibility for a $d = 3$ Ising model as a function of the applied magnetic field h for different values of R as found by a Monte Carlo simulation [7]. The temperature is taken to be $4T_c/9$, where T_c is the critical point temperature. The solid line is the mean-field prediction of the inverse susceptibility for $q \rightarrow \infty$, where q is the number of spins that interact with a given spin [37]. Data was taken only if the metastable state lived longer than 10^4 Monte Carlo time steps per spin. For nearest-neighbor interactions ($q = 6$) the data stops at $h \sim 0.5$ far from the spinodal value of the field $h_s = 1.43$. As R and hence q is increased, the data approaches the mean-field result and the spinodal can be more closely approached. This result indicates that the system behaves more like there is an underlying spinodal the larger the value of R .

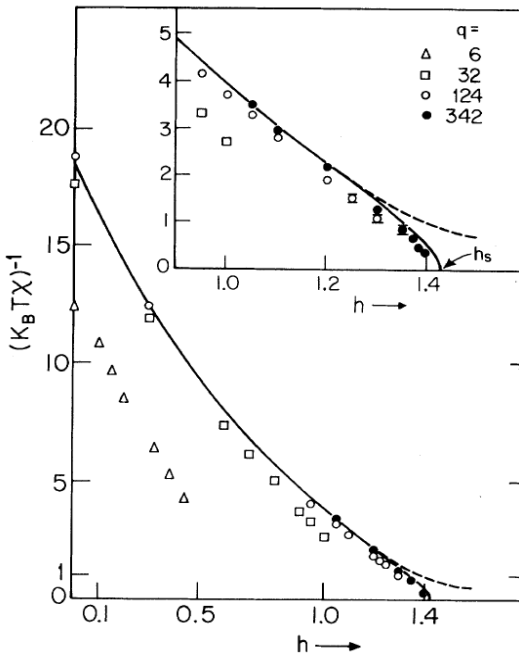


FIG. 1: The inverse susceptibility as a function of the magnetic field h (from Ref. [7]). Note that as the number of interactions q is increased, the inverse susceptibility more closely follows a power law. The inset shows the behavior of $(kT\chi)^{-1}$ closer to the pseudospinodal.

Another way to understand the meaning of the pseudospinodal is to look at the behavior of the zeros of the partition function in an Ising model as a function of the interaction range R . The zeros of the partition function corresponding to the spinodal lie in the four-dimensional complex magnetic field-temperature space for finite R [9]. As R is increased, the zeros move toward the real h, T plane similar to what occurs in the Lee-Yang study of zeros of the partition function for Ising models in finite systems [38, 39]. The point is that the pseudospinodal appears to be a critical point if h is not too close to h_s . What is meant by too close can be estimated by the Ginzburg parameter G_s in Eq. (57). The value of Δh where the spinodal concept begins to fail can be made smaller by increasing R . Hence, the theoretical arguments we made about the properties of fluctuations near the spinodal can be tested in systems where the interaction range R is large, even though there is no true spinodal in nature. However, such a statement has to be modified in systems with a phase transition that involve spatial symmetry breaking such as the liquid-solid transition (see Sec. VIII).

V. PERCOLATION MAPPING

To obtain a deeper understanding of the structure of the fluctuations near the mean-field critical point, we map the Ising critical point onto a percolation transition. We begin by asking if Ising critical points (mean-field or non-mean-field) can be mapped onto a percolation transition for a properly chosen percolation model [40]. To answer this question we first describe the mapping introduced by Kastaleyn and Fortuin [41] from the s -state Potts model onto random bond percolation. The random bond percolation model is defined on a lattice in d dimensions where all the sites or vertices are occupied with a probability of one, and the bonds are occupied with a probability p_b . Clusters are defined as a set of sites connected to each other by bonds and not connected to any other sites in the lattice. Cluster properties such as size are defined by the number of sites in the cluster [42].

The Hamiltonian for the s -state Potts model is

$$H_P = -J_P \sum_{ij} (\delta_{\sigma_i \sigma_j} - 1) - h_P (\delta_{\sigma_i 1} - 1), \quad (71)$$

where σ_i specifies the state of site i , $J_P > 0$ is the coupling constant, and h_P is the Potts field; the Kronecker delta $\delta_{\sigma_i \sigma_j}$ is nonzero only when two neighboring (that is, within the interaction range) sites are in the same state. For convenience we will set $h_P = 0$ for now. We can write the Boltzmann factor $e^{-\beta H_P}$ as

$$e^{-\beta H_P} = \prod_{ij} [\delta_{\sigma_i \sigma_j} + e^{-\beta J_P} (1 - \delta_{\sigma_i \sigma_j})], \quad (72)$$

or

$$e^{-\beta H_P} = \prod_{ij} [(1 - e^{-\beta J_P}) \delta_{\sigma_i \sigma_j} + e^{-\beta J_P}]. \quad (73)$$

We associate a bond with $\delta_{\sigma_i \sigma_j} = 1$ and the absence of a bond with $\delta_{\sigma_i \sigma_j} = 0$. With this association Kastaleyn and Fortuin [41] pointed out that the generating function for the random bond percolation model is obtained by differentiating the free energy for the s -state Potts model with respect to s and then setting s equal to 1. There are many subtle mathematical points in the Kastaleyn-Fortuin proof of this assertion. We will not consider them here, but refer the interested reader to Ref. [41] and the references cited therein. However, because it will be needed to understand the structure of fluctuations, we demonstrate how the connection between the Potts model and percolation works.

The partition function Z_P is given by

$$Z_P = \sum_{\sigma} e^{-\beta H_P}. \quad (74)$$

and the free energy in the canonical ensemble is

$$F_P(\beta, s) = -k_B T \ln Z_P. \quad (75)$$

If we differentiate $-\beta$ times the free energy with respect to s , we obtain

$$-\beta \frac{\partial F_P(\beta, s)}{\partial s} = \sum_{\sigma} \frac{1}{Z_P} \frac{\partial e^{-\beta H_P}}{\partial s}. \quad (76)$$

Setting $s = 1$ results in $H_P = 0$ because there is only one Potts state; hence $Z_P = s^N = 1$ for $s = 1$, where N is the number of sites in the lattice. Therefore

$$-\beta \frac{\partial F_P(\beta, s)}{\partial s} \Big|_{s=1} = \frac{\partial}{\partial s} \sum_{\sigma} e^{-\beta H_P} \Big|_{s=1}. \quad (77)$$

The percolation generating function is the right-hand side of Eq. (77) with $s = 1$. To understand this interpretation we will look at several terms in Eq. (77). We use Eq. (73) for $e^{-\beta H_P}$ and first consider the term $e^{-\beta J_P}$ in each of the factors in the product. That is, we include no terms with $\delta_{\sigma_i \sigma_j}$. For a lattice with N sites or vertices and coordination number c , selecting only those terms with $e^{-\beta J_P}$ and no delta functions results in a contribution to $F_P(\beta, s)$ of $s^N e^{-\beta J_P c N}$. By differentiating with respect to s and setting $s = 1$, we obtain a contribution to the generating function G_f of the form

$$G_{f,1} = N e^{-\beta J_P c N}. \quad (78)$$

Because there are N sites and cN bonds, $G_{f,1}$ can be interpreted as the mean number of single site clusters. That is, $e^{-\beta J_P c N}$ is the probability that there are no bonds present.

We now consider a term from Eq. (73) that includes only one delta function. Suppose that it is $\delta_{\sigma_1 \sigma_2}$. The contribution to the generating function G_f will be of the form

$$G_{f,2}(p) = (1 - e^{-\beta J_P}) s e^{-\beta J_P (cN-1)} s^{N-2} = p_b (1 - p_b)^{cN-1} s^{N-1}, \quad (79)$$

where we have associated the bond probability p_b with $1 - e^{-\beta J_P}$. Differentiating with respect to s and setting $s = 1$ gives $N - 1$ for the number of clusters times the probability of such a configuration. There are $N - 2$ one site clusters and one two site cluster for a particular

bond. The number of ways we can choose one bond is cN , so that the first two contributions to $\partial F(\beta, s)/\partial s$ are

$$G_{f,1}(p) + G_{f,2}(p) = N(1 - p_b)^{cN} + (N - 1)cNp_b(1 - p_b)^{cN-1}. \quad (80)$$

We could continue in this manner but the pattern is clear. The terms we obtain are the number of clusters in a given configuration. The complete enumeration of the configurations will lead to an expression for the mean number of clusters as a function of $p_b = 1 - e^{-\beta J_P}$. The mean number of clusters can be written as

$$G_f(p) = \sum_k \langle n_k \rangle, \quad (81)$$

where $\langle n_k \rangle$ is the mean number of clusters with k sites.

In order to obtain the full generating function for the random bond percolation problem, we must include the field h_P in the calculation of the free energy. We write

$$e^{-\beta H_P} = \prod_{ij} [(1 - e^{-\beta J_P})\delta_{\sigma_i \sigma_j} + e^{-\beta J_P}] \prod_l [(1 - e^{-\beta h_P})\delta_{\sigma_l 1} + e^{-\beta h_P}]. \quad (82)$$

The terms in the expansion of Eq. (82) represent sets of connected sites (clusters) generated by $\delta_{\sigma_i \sigma_j}$. Terms of the form $\delta_{\sigma_k 1}$, where the index 1 labels one of the s possible states of a site, will give no contribution to the derivative of the partition function with respect to s . The reason is that the $\delta_{\sigma_k 1}$ term fixes all spins in a cluster to the Potts state labeled as 1. Hence there is no s dependence and no factor of s in the product that will be s raised to the power of the number of clusters. From Eq. (82) all clusters with a nonzero weight after differentiating with respect to s will have a field dependence of the form $e^{-h_P m}$, where m is the number of sites in the cluster. If we resum as in Eq. (80). we obtain [41]

$$G_f(p_b, h_P) = \sum_k \langle n_k \rangle e^{-k\beta h_P}. \quad (83)$$

The reader might want to work out the generating function for small lattices to see precisely how the sum in Eq. (83) arises.

To investigate the mapping of the percolation model onto the Ising model, we consider the dilute s -state Potts [43] model with the Hamiltonian

$$\beta H_{DP} = -\beta J_P \sum_{ij} (\delta_{\sigma_i \sigma_j} - 1)n_i n_j - \beta h_P \sum_i (\delta_{\sigma_i 1} - 1)n_i - K_{LG} \sum_{ij} n_i n_j + \Delta \sum_i n_i. \quad (84)$$

Here J_P is the Potts coupling constant as before and h_P is the Potts field as in Eq. (82). The quantity n_i is the occupation number where $n_i = 1$ denotes that a particle or spin occupies site i and $n_i = 0$ denotes an empty site. Hence there is a Potts interaction between occupied ($n_i = 1$) sites. The quantity

$$\beta H_{LG} = -K_{LG} \sum_{ij} n_i n_j + \Delta \sum_i n_i \quad (85)$$

is the Hamiltonian for the lattice gas formulation of the Ising model [44], where K_{LG} is the (dimensionless) coupling constant and Δ is the chemical potential. In terms of the parameters in the Ising Hamiltonian H_I ,

$$\beta H_I = -K_I \sum_{ij} s_i s_j + \beta h_I \sum_i s_i \quad (86)$$

with $s_i = \pm 1$, we have [44]

$$K_{LG} = 4K_I \text{ and } \Delta = \beta h_I + 2cK_I. \quad (87)$$

Differentiating the free energy constructed from H_{DP} with respect to s and setting $s = 1$ results in the generating function for correlated site random bond percolation. This model has occupied sites distributed according to the lattice gas Hamiltonian in Eq. (85) and bonds thrown with a probability p_b between pairs of occupied sites. To understand this connection we note that

$$Z_{DP} = \sum_{\sigma_i \sigma_j n_i n_j} e^{-\beta H_{DP}}, \quad (88)$$

and

$$-\frac{\partial k_B T \ln Z_{DP}}{\partial s} \Big|_{s=1} = \frac{\frac{\partial}{\partial s} \left(\sum_{\{\sigma_i\}\{n_i\}} e^{\sum_{ij} \beta J_P (\delta_{\sigma_i \sigma_j} - 1) n_i n_j + \beta h_P \sum_i (\delta_{\sigma_i 1} - 1) n_i} \right) \Big|_{s=1} e^{-\beta H_{DP}}}{Z_{DP}}. \quad (89)$$

If we write

$$\exp [\beta J_P (\delta_{\sigma_i \sigma_j} - 1) n_i n_j] = [(1 - e^{-\beta J_P}) \delta_{\sigma_i \sigma_j} + e^{-\beta J_P}] n_i n_j + (1 - n_i n_j), \quad (90)$$

and

$$\exp [\beta h_P \sum_i (\delta_{\sigma_i 1} - 1) n_i] = (1 - e^{-\beta h_P}) \delta_{\sigma_i 1} n_i + e^{-\beta h_P} n_i + (1 - n_i), \quad (91)$$

we can use the same arguments that we gave previously for random percolation to show that the expression in Eq. (89) leads to the generating function for correlated site random bond

percolation where the occupied sites are distributed according to the lattice gas Boltzmann factor constructed from the Hamiltonian in Eq. (85) [43]. Note that for this model the sum over the s states of the Potts spin is one for all s if site i is empty, that is, if $n_i = 0$.

We now consider the Hamiltonian H_{DP} in Eq. (84). We set h_P and h_I equal to zero, and hence Δ reduces to $\Delta = 2qK_I = qK_{LG}/2$ from Eq. (87). In addition, in Eq. (84) we set $J_P = K_{LG}/2$. The dilute Potts Hamiltonian H_{DP} becomes

$$\beta H_{DP} = -\frac{K_{LG}}{2} \sum_{ij} (\delta_{\sigma_i \sigma_j} - 1) n_i n_j - K_{LG} \sum_{ij} n_i n_j + \frac{K_{LG}}{2} \sum_{ij} (n_i + n_j). \quad (92)$$

Suppose that for a pair of sites within the interaction range, either both sites are empty or both sites are filled, but the spins are in the same Potts state. Note that when both sites are empty, we have only one Potts configuration. For these configurations the contribution to $H_{DP} = 0$, and there are $s + 1$ configurations of the pair that give this contribution. Now consider the situation where either one site is occupied and one empty or both sites are occupied, but the spins are in different Potts states. In this case the contribution of this pair to H_{DP} is $K_{LG}/2$, and the number of ways this combination can be obtained is $(s + 1)s$. These considerations imply that the dilute s -state Potts model at $J_P = K_{LG}/2$ is equivalent to a pure $(s + 1)$ -state Potts model with the Hamiltonian

$$\beta H_{P,(s+1)} = -\frac{K_{LG}}{2} (\delta_{\sigma_i \sigma_j} - 1), \quad (93)$$

where σ_i can be in $s + 1$ states. However, the $s = 2$ Potts model is the lattice gas model in Eq. (84) with $\Delta = cK_{LG}/2$. That is, for $\beta J_P = K_{LG}/2 = 2K_I$ and $h_I = h_P = 0$, the Hamiltonian of the dilute s -state Potts model is the same as the Hamiltonian for the $(s + 1)$ -state pure Potts model. In the limit $s \rightarrow 1$, the $(s + 1)$ -state pure Potts model is the lattice gas model.

In this formulation we can write the Boltzmann factor as

$$e^{-\beta H_{P,(s+1)}} = \prod_{ij} [(1 - e^{-K_{LG}/2}) \delta_{\sigma_i \sigma_j} + e^{-K_{LG}/2}]. \quad (94)$$

We factor out $e^{-K_{LG}/2}$ and obtain

$$e^{-\beta H_{P,(s+1)}} = e^{-K_{LG}cN/2} \prod_{ij} \left[\frac{1 - e^{-K_{LG}/2}}{e^{-K_{LG}/2}} \delta_{\sigma_i \sigma_j} + 1 \right], \quad (95)$$

where N is the number of lattice sites.

Clearly the singular behavior of the free energy comes from the terms in Eq. (95) in the product over lattice sites. This product has the form of $\prod_{ij}[f_{ij} + 1]$, where we associate a graph or cluster with a product of the f_{ij} summed over Potts states. These clusters are the same as the percolation clusters because the sites are connected by $\delta_{\sigma_i\sigma_j}$ bonds. The linked cluster theorem [45, 46] implies that the singular part of the free energy $F_{P,\text{sing}}$ is the sum over all *connected* graphs in the thermodynamic limit. Connected graphs are those in which all points or vertices of the graph are connected by an f_{ij} bond. Because the graphs are connected, the sum over Potts states results in a factor of s , independent of the size or structure of the graph. Therefore the derivative of $F_{P,\text{sing}}$ with respect to s results in the same sum without the overall factor of s . Thus

$$2\frac{dF_{P,\text{sing}}}{ds}\bigg|_{s=1} = F_{P,\text{sing}}\bigg|_{s=1}, \quad (96)$$

which implies that the percolation transition and the Ising critical point are the same in that they occur at the same temperature and have the same critical exponents. The amplitudes of the singular quantities differ by a factor of two. If instead of the Hamiltonian in Eq. (84), which defines clusters as consisting of only occupied sites, we add a term to the Hamiltonian of the form

$$\begin{aligned} \beta H_{DP,\text{empty}} = & -\beta J_P \sum_{ij} (\delta_{\sigma_i\sigma_j} - 1)(1 - n_i)(1 - n_j) \\ & - K_{LG} \sum_{ij} (1 - n_i)(1 - n_j) + \Delta' \sum_i (1 - n_i), \end{aligned} \quad (97)$$

we can define clusters between “empty” sites. In this way the singular part of the free energy will be identical to the mean number of clusters for $s \rightarrow 1$ and $h_P = 0$. The same result was obtained using renormalization group techniques in Ref. [40].

We now consider the mapping of a thermal problem onto a percolation model near the spinodal. This mapping will require a slightly different approach. We again begin with the dilute s -state Potts model. The Hamiltonian is the sum of H_{DP} and H_{LG} , from Eqs. (84) and (85). This Hamiltonian can be put into a continuum form using the Gaussian transformation [32, 47]. Because we are interested in the mean-field limit, the Landau-Ginzburg-Wilson Hamiltonian is the Landau-Ginzburg free energy. We have from Refs. [25, 47]

$$\begin{aligned} F_{DP}(\zeta, \phi) = & \int d\mathbf{x} \left[\frac{1}{2} s(s-1) (R \nabla \zeta(\mathbf{x}))^2 - r_1 s(s-1) \zeta^2(\mathbf{x}) - h_P(s-1) \zeta(\mathbf{x}) \right. \\ & \left. + \frac{w_1}{4!} s(s-1)(s-2)(s-3) \zeta^3(\mathbf{x}) + \frac{w_2}{2} s(s-1) \zeta^2(\mathbf{x}) \phi(\mathbf{x}) \right] + F(\phi), \end{aligned} \quad (98)$$

where $F(\phi)$ is the Landau-Ginzburg-Wilson free energy in Eq. (50). The constants r_1 , w_1 , w_2 , and ϵ in Eq. (50) can be written as functions of J , K_{LG} , and the lattice coordination number c . The global percolation order parameter ζ is the probability that a spin in the stable phase direction belongs to the infinite cluster of occupied sites. As for of a discrete system, the percolation model is obtained by differentiating F_{DP} with respect to s and setting $s = 1$ [47].

In order to map the thermal problem near the spinodal onto the percolation problem, we rewrite Eq. (50) as in Eq. (54) which we repeat here for convenience.

$$F(\psi) = \int d\mathbf{x} \left[\frac{R^2}{2} (\nabla \psi(\mathbf{x}))^2 + \Delta h^{1/2} \lambda_1 \psi^2(\mathbf{x}) - \lambda_2 \psi^3(\mathbf{x}) + \lambda_3 \psi^4(\mathbf{x}) \right], \quad (99)$$

where $\Delta h = h_s - h_I$, and $\psi(\mathbf{x}) = \phi(\mathbf{x}) - \phi_s + a$; a is chosen so that there is no term linear in $\psi(\mathbf{x})$ in the free energy. The constants such as λ_1 are obtained from the transformation.

We equate the functional derivative of $dF_{\text{DP}}(\zeta, \phi)/ds|_{s=1} = F_{\text{P}}$ with respect to $\zeta(\mathbf{x})$ with the functional derivative of $F(\psi)$ with respect to ψ . That is,

$$\frac{\delta F_{\text{P}}}{\delta \zeta} = -R^2 \nabla^2 \zeta(\mathbf{x}) - 2r_1 \zeta(\mathbf{x}) + \frac{w_1}{3} \zeta^2(\mathbf{x}) + w_2 \zeta(\mathbf{x}) \phi(\mathbf{x}) - h_{\text{P}}, \quad (100)$$

and

$$\frac{\delta F(\psi)}{\delta \psi} = -R^2 \nabla^2 \psi(\mathbf{x}) + 2\lambda_1 \Delta h^{1/2} \psi(\mathbf{x}) - 3\lambda_2 \psi^2(\mathbf{x}) + 4\lambda_3 \psi^3(\mathbf{x}) \quad (101)$$

must be equal. This condition implies that $-2(r_1 - \frac{w_2}{2} \phi_s) \zeta + \frac{w_1}{3} \zeta^2 - h_{\text{P}}$ must be the same as $2\lambda_1 \Delta h^{1/2} \psi - 3\lambda_2 \psi^2$. We dropped the ψ^3 term in the Euler-Lagrange equation because $\psi \sim \Delta h^{1/2} \ll 1$ as we will see in Secs. VI and XI.

Hence at the spinodal ($\Delta h = 0$) we identify ζ with $-\psi$ and require that $h_{\text{P}} = 0$, $w_1/3 = -3\lambda_2$, and $r_1 = w_2 \phi(\mathbf{x})/2$. With these equalities the solutions of Eqs. (100) and (101) with $\delta F_{\text{P}}/\delta \zeta(\mathbf{x}) = \delta F(\psi)/\delta \psi(\mathbf{x}) = 0$ are identical. If we write the parameters in Eqs. (100) and (101) in terms of the parameters J_{P} , K_{LG} , and c of H_{DP} in Eqs. (84) and (85), we obtain

$$\beta J_{\text{P}} = 2K_I(1 - \rho), \quad (102)$$

where the density $\rho = (1 + m)/2$ and ϕ is proportional to m , the magnetization per spin. Because we are interested in the coincidence of the spinodal with a percolation transition, we can set $\phi(\mathbf{x}) = \phi_s$, the value of the order parameter at the spinodal.

To define the bond probability in terms of a physically meaningful quantity, we need to obtain the proportionality factor between ϕ_s and m_s , the value of the magnetization at the

spinodal. To do so we use the relation between the Ising model and the continuum ϕ^4 theory generated by the Hubbard-Stratonovich transformation [32]. In particular, the value of ϕ at the spinodal is [47]

$$\phi_s = \pm \frac{[(cK_I - 1)c]^{1/2}}{c^2 K_I}. \quad (103)$$

When $T \rightarrow 0$ or equivalently $K_I \rightarrow \infty$, the value of m_s must approach 1 as can be seen if we remember that the magnetic field is divided by T in the Boltzmann factor. Because $\phi_s \rightarrow 1/cK_I^{1/2}$ as $K_I \rightarrow \infty$, we have

$$m_s = cK_I^{1/2} \phi_s, \quad (104)$$

so that $m_s \rightarrow 1$ as $K_I \rightarrow \infty$. If we use Eq. (104), we obtain the expression for the bond probability that maps the percolation model onto the spinodal

$$p_b = 1 - e^{-\beta J_P}, \quad (105)$$

where J_P is given in Eq. (102). The validity of this mapping was demonstrated numerically in Refs. [10, 12, 48].

The interpretation of this mapping is that the spinodal curve is the locus of a set of percolation transitions. If the spinodal curve is approached off-critical with $h \neq 0$, there is a transition to a spanning cluster in the stable phase direction at the spinodal. Although it has been stated several times, we stress that this result is only correct in the mean-field ($G_s \rightarrow \infty$) limit.

The various mappings we have discussed imply that the free energy of the lattice gas model is isomorphic to the generating function for correlated site random bond percolation. For $h_P = h_I = 0$, the generating function is the mean number of clusters.

VI. FLUCTUATION STRUCTURE

In this section we will use scaling arguments to obtain information about the structure of fluctuations in mean-field and near-mean-field systems. We will revisit these scaling arguments in Sec. VII where we apply the Parisi-Sourlas technique.

From the mappings presented in Sec. V we see that the quantity that is isomorphic to the free energy in a correlation length volume is $-k_B T$ times the mean number of clusters in a correlation length volume. The free energy per spin or particle at the critical value of

the field or chemical potential scales as ϵ^2 , because the specific heat exponent $\alpha = 0$ near mean-field critical points [33, 34]. Hence the free energy $F(\epsilon)$ in a correlation length volume scales as

$$F(\epsilon) \sim \epsilon^2 \xi^d = R^d \epsilon^{2-d/2} = G, \quad (106)$$

and hence from the discussion in Sec. V the number of clusters in a correlation length volume scales as in Eq. (106). The value of the free energy at the minimum is the negative of $F(\epsilon)$ in Eq. (106). We will discuss this point again in Sec. VII (see Eq. (131)).

How are the clusters related to the fluctuations? In non-mean-field systems such as the Ising model with short-range interactions and $d < 4$, the mean number of clusters (in a correlation length volume) near the critical point is $\epsilon^{2-\alpha} \xi^d \sim 1$. This result follows from $\xi \sim \epsilon^{-\nu}$ and the hyperscaling relation $d\nu = 2 - \alpha$ [33, 34]. The isomorphism between percolation and the thermal system implies that the pair connectedness function is the same as the pair distribution function. The pair connectedness function is the probability that two spins a distance x apart belong to the same cluster. For a distance less than the correlation length ξ , the probability that two spins belong to the same cluster is roughly a constant and equal to the square of the density of spins in the cluster ρ_{cl}^2 . This density must be equal to the density of a fluctuation which scales as ϵ^β [33, 34]. Hence, the density of spins in a cluster in a system with short-range interactions scales as ϵ^β , and the clusters are a statistical realization of the fluctuations [40, 42].

In mean-field and a near-mean-field systems the number of clusters in a correlation length volume near the critical point scales as $G = R^d \epsilon^{2-d/2}$ (see Eq. (106)), which is much larger than one. Are the clusters a statistical realization of the fluctuations? To understand that the answer is no, we note that the fluctuation density from Eq. (17) scales as $\phi(\mathbf{x}) \sim \epsilon^{1/2} / (R^d \epsilon^{2-d/2})^{1/2}$. If a single cluster were to correspond to a fluctuation, then the density of spins ρ_{spin} (or particles) in a correlation length volume would be (see Eqs. (9a) and (17))

$$\rho_{\text{spin}} \sim \xi^d \phi(\mathbf{x}) = R^d \epsilon^{2-d/2} \frac{\epsilon^{1/2}}{[R^d \epsilon^{2-d/2}]^{1/2}} = [R^d \epsilon^{2-d/2}]^{1/2} \epsilon^{1/2}. \quad (107)$$

Because the mean-field limit is taken by letting $R \rightarrow \infty$ before $\epsilon \rightarrow 0$ [5], the scaling in Eq. (107) would imply that the spin density is infinite in the mean-field limit, which is not possible. Hence, the density of the clusters is much smaller than the density of the fluctuations in mean-field and near-mean-field systems, and a fluctuation does not correspond to a single cluster as it does in short-range systems. We conclude that the clusters in mean-field

and near-mean-field systems play a different role, and we will refer to the clusters in these systems as *fundamental clusters*.

To understand the relation between the clusters and fluctuations in the mean-field limit, we note that the integral of the pair distribution function minus the square of the density is the isothermal susceptibility. That is

$$\chi_T \propto \int d\mathbf{x} [\rho^{(2)}(\mathbf{x}) - \rho^2]. \quad (108)$$

For a system with short-range interactions the hyperscaling relation $d\nu = 2 - \alpha$ is valid [33, 34], and we can use scaling arguments to show that χ_T in Eq. (108) scales as [49]

$$\chi_T \sim \epsilon^{2\beta} \xi^d = \epsilon^{2\beta - d\nu}. \quad (109)$$

Because $2\beta + \gamma = 2 - \alpha$ and $d\nu = 2 - \alpha$, we have that $2\beta - d\nu = -\gamma$ [33, 34].

In a mean-field or near-mean-field system we have from Eqs. (17) and (108)

$$\chi_T \sim \left[\frac{\epsilon^{1/2}}{(R^d \epsilon^{2-d/2})^{1/2}} \right]^2 R^d \epsilon^{-d/2} = \epsilon^{-1} \quad (110)$$

as expected [33, 34].

As we have discussed, the mapping onto the percolation model implies that the pair distribution function is the same as the pair connectedness function. Because the latter is the probability that two sites a distance x apart belong to the same cluster, we have from a scaling perspective (for two sites within a correlation length)

$$\rho_{\text{cl}}^{(2)}(\mathbf{x} \ll \xi) \sim \frac{\rho_{\text{cl}}^2}{R^d \epsilon^{2-d/2}}. \quad (111)$$

The quantity ρ_{cl} is equal to the probability that a site belongs to any one of the $R^d \epsilon^{2-d/2}$ clusters; $\rho_{\text{cl}}/R^d \epsilon^{2-d/2}$ is the probability that another site belongs to the same cluster as the first.

As before, the clusters have a linear spatial extent equal to the correlation length, and we expect that the probability of two sites belonging to the same cluster to be a constant for $x \ll \xi$. Because the pair connectedness function and the pair distribution function are isomorphic to each other, we must have (see Eq. (16))

$$\frac{\rho_{\text{cl}}^2}{R^d \epsilon^{2-d/2}} = \left[\frac{\epsilon^{1/2}}{(R^d \epsilon^{2-d/2})^{1/2}} \right]^2, \quad (112)$$

or $\rho_{\text{cl}} = \epsilon^{1/2}$. Hence, the density of spins in a fundamental cluster is

$$\rho_{\text{cl}}(\mathbf{x} \ll \xi) \sim \frac{\epsilon^{1/2}}{R^d \epsilon^{2-d/2}}. \quad (113)$$

We can test the prediction for $\rho_{\text{cl}}(\mathbf{x})$ in Eq. (113) by determining the dependence of the mean number of spins in a fundamental cluster m_{cl} on ϵ . This dependence is given by

$$m_{\text{cl}} \sim \frac{\epsilon^{1/2}}{R^d \epsilon^{2-d/2}} R^d \epsilon^{-d/2} = \epsilon^{-3/2}. \quad (114)$$

In Fig. 2 we plot the mean number of spins in a fundamental cluster as a function of ϵ for fixed R . The slope of the log-log plot is consistent with the theoretical prediction in Eq. (114).

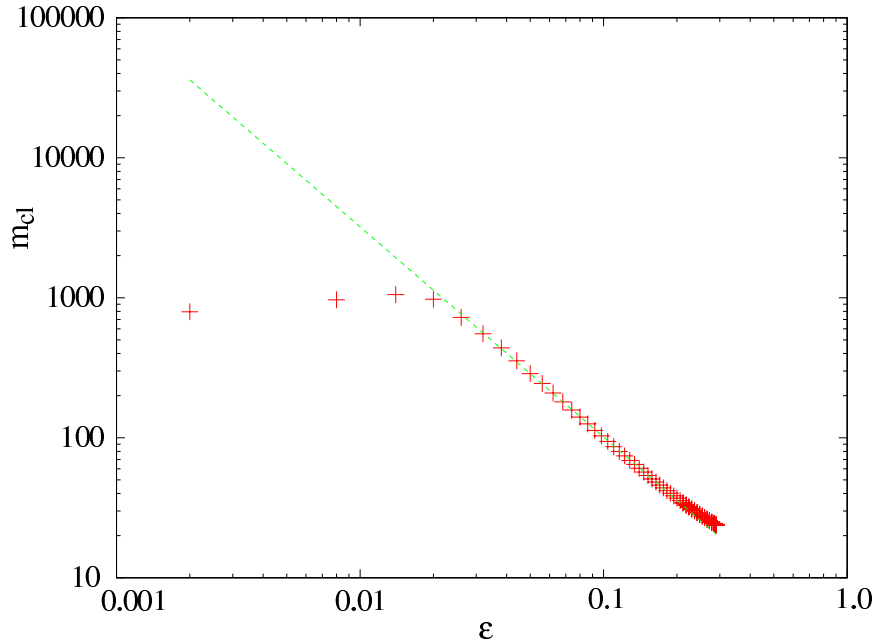


FIG. 2: The mean number of spins in a fundamental cluster found in a Monte Carlo simulation of the two-dimensional long-range Ising model with $R = 20$ near T_c as a function of ϵ . The linear dimension of the system is $L = 240$. The slope is -1.5 if the data is fitted in the range $[0.03, 0.2]$. Note the deviation of m_{cl} from the mean-field prediction near the pseudospinodal. For this range of ϵ , G is too small to apply mean-field arguments.

We have argued that because the density of the fundamental clusters is much smaller than the density of the fluctuations in mean-field and near-mean-field systems, a fluctuation must correspond to many fundamental clusters. We now discuss the relation between fundamental clusters and fluctuations in more detail. The clusters as given by the mappings

discussed in the Sec. V are constructed to be independent. Therefore a given cluster can “flip” independently of the remaining clusters. There are $R^d \epsilon^{2-d/2}$ clusters near the mean-field critical point, half of which are up and half down by symmetry. Because the clusters are independent, the mean number of excess fundamental clusters in a given direction will be

$$\overline{\Delta N}_{\text{fc}, \text{c}} \sim [R^d \epsilon^{2-d/2}]^{1/2} = G_s. \quad (115)$$

More precisely, the distribution of the number of fundamental clusters in a fluctuation is a Gaussian sharply peaked about $\overline{\Delta N}_{\text{fc}, \text{c}}$.

From this analysis the density of a fluctuation is the product of the density of fundamental clusters, Eq. (113), and the mean number of excess clusters, Eq. (115):

$$\phi(\mathbf{x}) \sim \frac{\epsilon^{1/2}}{R^d \epsilon^{2-d/2}} (R^d \epsilon^{2-d/2})^{1/2} = \frac{\epsilon^{1/2}}{(R^d \epsilon^{2-d/2})^{1/2}} = \frac{\epsilon^{1/2}}{G_s^{1/2}}, \quad (116)$$

in agreement with Eq. (17).

A similar analysis can be done near the spinodal. In this case there is an infinite cluster that is a statistical realization of the metastable state magnetization or density [23, 24]. If we subtract this cluster [51], the situation is similar to what occurs at the mean-field critical point. Namely, there are $R^d \Delta h^{3/2-d/4}$ fundamental clusters in a correlation length volume, half up and half down. The density of the fundamental clusters near the spinodal is obtained using the same arguments employed at the critical point. The mean number of fundamental clusters is given by (compare to Eq. (106))

$$\overline{N}_{\text{fc}, \text{s}} \sim R^d \Delta h^{3/2-d/4} = G_s, \quad (117)$$

and their density is

$$\psi \sim \frac{\Delta h^{1/2}}{R^d \Delta h^{3/2-d/4}} = \frac{\Delta h^{1/2}}{G_s}. \quad (118)$$

Hence, the density of the fluctuations scales as

$$\psi(\mathbf{x} \ll \xi) \sim \frac{\Delta h^{1/2}}{(R^d \Delta h^{3/2-d/4})^{1/2}} = \frac{\Delta h^{1/2}}{G_s^{1/2}}. \quad (119)$$

As we saw in Eqs. (11) and (57) the conditions $G = R^d \epsilon^{2-d/2} \gg 1$ and $G_s = R^d \Delta h^{3/2-d/4} \gg 1$ are the criteria for near-mean-field behavior. From our analysis of the fundamental clusters we see that a system is near-mean-field when the number of fundamental clusters in a correlation length volume is large (see Eq. (117)). As ϵ or Δh is decreased

for $d < 4$ (critical point) or $d < 6$ (spinodal) for R fixed, G and G_s decrease and the system becomes less mean-field. In systems that are not mean-field or near-mean-field, we have hyperscaling if Δh is sufficiently small, or, in simple fluids and magnets, we have two exponent scaling [33, 34]. This connection suggests that the quantities G or G_s determine the existence of two exponent scaling. Specifically, if G or G_s decreases, the clusters must coalesce and additional length scales are introduced [52].

Suppose for the moment that there is only one relevant or divergent length near the mean-field critical point. We will show that the assumption of one divergent length scale is insufficient for the existence of two exponent scaling in mean-field and near-mean-field systems because the number of fundamental clusters changes as the mean-field critical point is approached. The assumption of one divergent length scale leads to the following scaling form for the singular part of the free energy per spin (or particle) near the critical point [33, 34]

$$f(\epsilon, h) = \frac{1}{\xi^d} f(\xi^{y_T} \epsilon, \xi^{y_h} h). \quad (120)$$

If we differentiate f twice with respect to h and set $h = 0$, we find

$$\frac{\partial^2 f(\epsilon, h)}{\partial h^2} \Big|_{h=0} = \frac{\xi^{2y_h}}{\xi^d} \frac{\partial^2}{\partial (\xi^{y_h})^2} f(\xi^{y_T} \epsilon, \xi^{y_h} h) \Big|_{h=0}. \quad (121)$$

The left-hand side of Eq. (121) is the isothermal susceptibility. We now fix $\xi^{y_T} \epsilon$ to be equal to one. Because $f(1, h = 0)$ is not singular [33, 34], and $\xi \sim \epsilon^{-1/y_T}$, we have $\xi^{2y_h - d} = \epsilon^{-(2y_h - d)/y_T}$. We conclude that the critical exponent γ that characterizes the divergence of the isothermal susceptibility near the critical point is given by

$$\gamma = \frac{2y_h - d}{y_T}. \quad (122)$$

By using a similar argument, we obtain

$$\beta = \frac{d - y_h}{y_T}. \quad (123)$$

For mean-field Ising models or simple fluids $\beta = 1/2$ and $\gamma = 1$. Hence $y_h = 3d/4$ and $y_T = d/2$. However, for fixed, $R \xi = R \epsilon^{-1/2}$ so that $y_T = 2$ for all d [33, 34] and not $d/2$. We see that for fixed R two exponent scaling is not correct in the neighborhood of a mean-field critical point. The same argument can be made near the spinodal.

In contrast, consider what happens when $G = R^d \epsilon^{2-d/2}$ is held constant. From Eqs. (17) and (108) we have

$$\chi_T \sim \left[\frac{\epsilon^{1/2}}{(R^d \epsilon^{2-d/2})^{1/2}} \right]^2 R^d \epsilon^{-d/2}. \quad (124)$$

If we keep $R^d \epsilon^{2-d/2}$ constant, then

$$R^d \epsilon^{-d/2} \propto \epsilon^{-2}. \quad (125)$$

Therefore the susceptibility $\chi_T \propto \epsilon^{-1}$ so $\gamma = 1$. Likewise from Eq. (116) the density scales as $\epsilon^{1/2}$ so $\beta = 1/2$. Also from Eq. (125) $R\epsilon^{-1/2} \propto \epsilon^{-2/d}$ so that $\nu = 2/d$ and $y_T = d/2$. Two exponent scaling is now correct and $\gamma + 2\beta = d\nu$ so that hyperscaling is restored for fixed G . As is usually the case, the same arguments can be made near the spinodal with the caveat that the infinite cluster must be removed.

In summary we have shown that the relation between the clusters and the fluctuations in mean-field and near-mean-field systems is more complex than in systems with short-range interactions. In systems with long-range interactions the individual clusters are not realizations of the fluctuations and the latter is related to fluctuations of the number of clusters. We will refer to the clusters in mean-field and near-mean-field systems as fundamental clusters. The mean number of fundamental clusters or the Ginzburg parameter is a function of ϵ (Δh) near the critical point (spinodal). The dependence of the Ginzburg parameter G on ϵ (G_s on Δh) causes the breakdown of two exponent scaling and hyperscaling.

VII. FLUCTUATION STRUCTURE: LANDAU-GINZBURG AND PARISI-SOURLAS

In Sec. VI we assumed a scaling form for the free energy. In this section we do a more detailed calculation using the Landau-Ginzburg-Wilson Hamiltonian in the mean-field limit. In addition to recovering the same scaling results, we will also determine the scaling dependence of the lifetime of the fundamental clusters.

The partition function is given by

$$Z = \int \delta\phi(\mathbf{x}) \exp \left\{ -\beta \int d\mathbf{x} \left[R^2 \frac{(\nabla\phi(\mathbf{x}))^2}{2} + \epsilon\phi^2(\mathbf{x}) + \phi^4(\mathbf{x}) - h\phi(\mathbf{x}) \right] \right\}. \quad (126)$$

If we set $h = 0$, scale all lengths with the correlation length, and assume that $\phi(\mathbf{x})$ scales as $\epsilon^{1/2}$ near the critical point, we obtain the Hamiltonian in Eq. (8), which we rewrite here for convenience.

$$H(\phi) = R^d \epsilon^{2-d/2} \int d\mathbf{y} \left[\frac{(\tilde{\nabla}\tilde{\phi}(\mathbf{y}))^2}{2} \pm \tilde{\phi}^2(\mathbf{y}) + \tilde{\phi}^4(\mathbf{y}) \right], \quad (127)$$

where the $+$ ($-$) sign corresponds to $\epsilon > 0$ ($\epsilon < 0$). We now assume that $\tilde{\phi}(\mathbf{y})$ is independent of \mathbf{y} and restrict the integral to a region the size of a correlation length volume. We have

$$H(\phi) = R^d \epsilon^{2-d/2} [\pm \tilde{\phi}^2 + \tilde{\phi}^4]. \quad (128)$$

and the partition function becomes

$$Z(\epsilon) = \int_{-\infty}^{\infty} d\tilde{\phi} e^{-\beta R^d \epsilon^{2-d/2} (\pm \tilde{\phi}^2 + \tilde{\phi}^4)}. \quad (129)$$

For $R^d \epsilon^{2-d/2} \gg 1$ we can do the integral in Eq. (129) using saddle point techniques. For $\epsilon < 0$ the saddle points are at $\phi = \pm 1/\sqrt{2}$. In the limit $R^d \epsilon^{2-d/2} \gg 1$ we have

$$Z(\epsilon) \propto e^{\beta R^d \epsilon^{2-d/2}}, \quad (130)$$

and hence the free energy is

$$-k_B T \ln Z(\epsilon) = -R^d \epsilon^{2-d/2}, \quad (131)$$

where we have neglected the logarithmic corrections generated by the steepest descent integral. (Note the minus sign on the right-hand side of Eq. (131).) If $\epsilon > 0$, the saddle points are at $\pm i/\sqrt{2}$ and the free energy is also proportional to $-R^d \epsilon^{2-d/2}$. Hence, as assumed in Sec. VI, the number of fundamental clusters scales as $R^d \epsilon^{2-d/2}$ near the critical point. As usual, the same argument can be used near the spinodal for $G_s \rightarrow \infty$ and near the pseudospinodal for $G_s \gg 1$ in near-mean-field systems.

To obtain the lifetime of the fundamental clusters, we return to the Parisi-Sourlas method. From Eq. (43) we see that the lifetime of the fundamental clusters near the mean-field critical point is

$$\tau_{fc,c} \sim \frac{\epsilon^{-1}}{R^d \epsilon^{2-d/2}} \quad (\text{fundamental cluster lifetime near critical point}) \quad (132)$$

At the spinodal we have from Eq. (69)

$$\int d\mathbf{x} dt \left(\frac{\partial \psi}{\partial t} \right)^2 \sim 1. \quad (133)$$

From Eq. (118) we have

$$\psi(\mathbf{x} \ll \xi) \sim \frac{\Delta h^{1/2}}{R^d \Delta h^{3/2-d/4}}, \quad (134)$$

where we have taken the spatial extent of the fundamental cluster to be the correlation length. The lifetime of a fundamental cluster is found by requiring that

$$\frac{(\Delta h^{1/2})^2 R^d \Delta h^{d/4}}{\tau_{fc,s} [R^d \Delta h^{3/2-d/4}]^2} \sim 1, \quad (135)$$

or

$$\tau_{fc,s} \sim \frac{\Delta h^{-1/2}}{R^d \Delta h^{3/2-d/4}}. \quad (\text{fundamental cluster lifetime near spinodal}) \quad (136)$$

We see that near both the critical point and the spinodal in mean-field and near-mean-field systems where $R^d \epsilon^{2-d/2}$ and $R^d \Delta h^{3/2-d/4}$ are large, the lifetime of the fundamental clusters is considerably shorter than the lifetime (decorrelation time) of a fluctuation near the critical point (ϵ^{-1}) and the spinodal ($\Delta h^{-1/2}$).

To understand the relation between the lifetime of the fundamental clusters and the lifetime of a critical phenomena fluctuation (critical slowing down) we recall that the clusters are independent. We consider the fluctuations to be formed from the “vacuum” (zero magnetization near the critical point and zero net magnetization after the infinite cluster is subtracted near the spinodal or pseudospinodal) by a random walk in the number of fundamental clusters. At the critical point the critical phenomena fluctuations have a density (see Eq. (17))

$$\phi(\mathbf{x}) \sim \frac{\epsilon^{1/2}}{(R^d \epsilon^{2-d/2})^{1/2}}. \quad (137)$$

Because the fluctuations arise from a random walk in the number of fundamental clusters, there must be a “walk” of $(R^d \epsilon^{2-d/2})^{1/2}$ cluster flips (steps) in the direction of the fluctuation to obtain a density of

$$\phi(\mathbf{x}) \sim \frac{\epsilon^{1/2}}{R^d \epsilon^{2-d/2}} (R^d \epsilon^{2-d/2})^{1/2} = \frac{\epsilon^{1/2}}{(R^d \epsilon^{2-d/2})^{1/2}}. \quad (138)$$

To obtain a walk of this magnitude, there must be $R^d \epsilon^{2-d/2}$ attempted cluster flips. The time needed for this number of attempts is

$$\tau_{f,c} \sim \frac{\epsilon^{-1}}{R^d \epsilon^{2-d/2}} R^d \epsilon^{2-d/2} = \epsilon^{-1}, \quad (139)$$

in agreement with Eq. (38). The same considerations near the spinodal and the pseudospinodal yield

$$\tau_{f,s} \sim \Delta h^{-1/2} \quad (140)$$

for the lifetime of a fluctuation. The result (140) agrees with our earlier result for $\tau_{f,s}$ in Eq. (70).

In summary, we have argued that the fluctuations near mean-field critical points and spinodals can be represented by fundamental clusters in a suitably chosen percolation model. The relation between the fundamental clusters and fluctuations is qualitatively different

than that which exists between clusters and fluctuations in non-mean-field systems, that is, systems that obey hyperscaling. In mean-field and near-mean-field systems the fluctuations are formed by a random walk in the number of fundamental clusters that “flip” on a time scale considerably shorter than the scale set by critical slowing down.

In Secs. VIII–X we will explore some of the physical consequences of this fluctuation structure. The results discussed in the next three sections and other results that we will briefly describe in Sec. XI suggest that it is useful to interpret the fundamental clusters as actual physical objects and not merely a mathematical construct.

VIII. CLUSTER STRUCTURE AND INSTABILITIES IN SUPERCOOLED LIQUIDS

We begin our examination of the implications of the fluctuation structure on physical phenomena in mean-field and near-mean-field systems by discussing the physical implications of the fluctuation structure near the instability or liquid-solid spinodal in supercooled fluids. To explain the role of the structure of the fluctuations we first need to provide some background. In 1951 Kirkwood [53] noted that approximate equations for the distribution functions in the liquid state appeared to show an instability as the supercooled liquid is quenched deeper. Kirkwood began with the first equation of the static BBGKY hierarchy [54]

$$-k_B T \nabla_1 \ln \rho^{(1)}(\mathbf{x}_1) = \int d\mathbf{x}_2 \nabla_1 V(x_{12}) \frac{\rho^{(2)}(\mathbf{x}_1, \mathbf{x}_2)}{\rho^{(1)}(\mathbf{x}_1)}, \quad (141a)$$

or

$$-k_B T \nabla_1 \rho^{(1)}(\mathbf{x}_1) = \int d\mathbf{x}_2 \nabla_1 V(x_{12}) \rho^{(2)}(\mathbf{x}_1, \mathbf{x}_2), \quad (141b)$$

where $\rho^{(1)}(\mathbf{x}_1)$ and $\rho^{(2)}(\mathbf{x}_1, \mathbf{x}_2)$ are the one and two particle distribution functions respectively, ∇_1 denotes differentiation with respect to the position of particle 1, and $V(x_{12})$ is the interaction potential, which is assumed to be pairwise additive and spherically symmetric. Suppose that the system is in the liquid phase where the single particle distribution function is a constant equal to ρ , and the pair distribution function is a function of $x_{12} = |\mathbf{x}_1 - \mathbf{x}_2|$ and is equal to $\rho^2 h(x_{12}) = \rho^2(1 + g(x_{12}))$, where $g(x_{12})$ is the pair correlation function [54]. We substitute $\rho^{(1)}(\mathbf{x}_1) = \rho + \omega(\mathbf{x}_1)$ into Eq. (141b), treat $\omega(\mathbf{x}_1)$ as a small perturbation, and

linearize Eq. (141b) to find

$$-k_B T \frac{\nabla_1 \omega(\mathbf{x}_1)}{\rho} = \int d\mathbf{x}_2 \nabla_1 V(x_{12}) h(x_{12}) \omega(\mathbf{x}_2), \quad (142)$$

where the spherical symmetry of $V(x_{12})$ and $h(x_{12})$ results in

$$\int d\mathbf{x}_2 \nabla_1 V(x_{12}) h(x_{12}) = 0. \quad (143)$$

We have also assumed that a possible instability in $h(x_{12})$ is higher order in ω . We will return to this point later. If we define

$$q(\mathbf{x}_1 - \mathbf{x}_2) = \nabla_1 V(x_{12}) h(x_{12}), \quad (144)$$

we see that there is an instability [53] if there is a nonzero solution to

$$k_B T \nabla_1 \omega(\mathbf{x}_1) + \beta \rho \int d\mathbf{x}_2 q(\mathbf{x}_1 - \mathbf{x}_2) \omega(\mathbf{x}_2) = 0. \quad (145)$$

Kirkwood [53] analyzed Eq. (145) for the hard sphere fluid and concluded that there was an instability in $d = 3$. However, Kirkwood ignored the possible instability in $h(x_{12})$ which is connected through the BBGKY [54] hierarchy to possible instabilities in all of the distribution functions. Hence, it is not clear that the instability Kirkwood found is real. A more careful analysis done by Lovett [55] suggests that there is no instability in the hard sphere fluid, that is, the instability appears to vanish when higher order terms are considered.

In order to investigate the existence of an instability and its relation to a possible spinodal, Grewe and Klein [56, 57] investigated the properties of a simple fluid for which the interaction potential has the form assumed by Kac et al. [5] and is given by Eq. (1) with $V_R = 0$ and

$$\Phi(\gamma|\mathbf{x}|) = \begin{cases} 1 & \text{if } \gamma|\mathbf{x}| \leq 1, \\ 0 & \text{if } \gamma|\mathbf{x}| > 1. \end{cases} \quad (146)$$

In the mean-field limit $\gamma \rightarrow 0$, Grewe and Klein [56, 57] showed that all distribution functions of higher order than two are completely specified by only the single particle and pair distribution functions. The single particle distribution function in the limit $\gamma \rightarrow 0$ satisfies the equation

$$\rho^{(1)}(\mathbf{x}_1) = z \exp[-\beta \int d\mathbf{x}_2 \Phi(|\mathbf{x}_{12}|) \rho^{(1)}(\mathbf{x}_2)], \quad (147)$$

where $z = e^{-\beta\mu}$ and μ is the chemical potential. The pair correlation function satisfies

$$g(|\mathbf{x}_{12}|) = \beta \rho \Phi(|\mathbf{x}_{12}|) - \beta \rho \int d\mathbf{x}_3 g(|\mathbf{x}_1 - \mathbf{x}_3|) \Phi(|\mathbf{x}_2 - \mathbf{x}_3|), \quad (148)$$

where all length scales are in units of $\gamma^{-1} = R$. Note that $g(|\mathbf{x}_{12}|)$ is of order γ^d . The derivations of Eqs. (147) and (148) are beyond the scope of this paper, and the details are available in Refs. [56, 57].

From Eq. (148) the structure function $S(|\mathbf{k}|)$, which is obtained by taking the Fourier transform of $g(|\mathbf{x}_{12}|)$, is proportional to

$$S(|\mathbf{k}|) \propto \frac{1}{1 + \beta\rho\hat{\Phi}(|\mathbf{k}|)}, \quad (149)$$

where $\hat{\Phi}(|\mathbf{k}|)$ is the Fourier transform of $\Phi(\gamma|\mathbf{x}|)$. Note that the structure function is order one in the $\gamma \rightarrow 0$ limit.

We can perform a stability analysis on Eq. (147) similar to what was done by Kirkwood with the first BBGKY equation. We assume

$$\rho^{(1)}(\mathbf{x}_1) = \rho + \omega(\mathbf{x}_1), \quad (150)$$

where ρ is a constant and $\omega(\mathbf{x}_1)$ is a perturbation. We substitute Eq. (150) into Eq. (147) and linearize in $\omega(\mathbf{x}_1)$ to obtain

$$\omega(\mathbf{x}_1) = -\beta\rho \int d\mathbf{x}_2 \Phi(|\mathbf{x}_1 - \mathbf{x}_2|) \omega(\mathbf{x}_2), \quad (151)$$

where ρ is the solution of

$$\rho = z \exp[-\beta\hat{\Phi}(0)\rho], \quad (152)$$

and

$$\hat{\Phi}(0) = \int d\mathbf{x} \Phi(|\mathbf{x}|) > 0 \quad (153)$$

for the potential in Eq. (146). There is an instability only if there is a nonzero solution to Eq. (151). If we take the Fourier transform of Eq. (151), we can express the instability condition as

$$1 + \beta\rho\hat{\Phi}(|\mathbf{k}|) \leq 0, \quad (154)$$

or $\hat{\Phi}(|\mathbf{k}|) < 0$ for some value of $|\mathbf{k}|$ in order to have an instability. This condition is satisfied for the potential in Eq. (146). Because this choice of $\Phi(\gamma|\mathbf{x}|)$ has a Fourier transform which is bounded from below, there will be a value of $\beta\rho$ below which there is no instability. If $|\mathbf{k}| = k_0$ is the location of the global minimum of the Fourier transform of the potential, then the system has no instability for $\beta\rho < -1/\hat{\Phi}(k_0)$. We set $|\mathbf{k}| = k_0$ and see from Eq. (149) that the structure function $S(k_0)$ diverges for fixed ρ at the same value of the

temperature T at which an instability first appears. The divergence of $S(k_0)$ implies that the instability in the mean-field system is a spinodal. This divergence of $S(k_0)$ for $k_0 \neq 0$ is analogous to the divergence of the susceptibility at the Ising spinodal and the divergence of the compressibility at the liquid-gas spinodal.

In the mean-field limit there are no higher order distribution functions that need to be considered and the results of Grewe and Klein [56, 57] are rigorous. The structure function $S(k_0)$ diverges as $(T - T_s)^{-1}$ so that the critical exponent is the same as the Ising spinodal if the temperature rather than the magnetic field is used to approach the spinodal in the Ising model. The only difference is that in gases and Ising models the structure function diverges at $|\mathbf{k}| = 0$ rather than at $k_0 \neq 0$ corresponding to the liquid-solid spinodal. The other critical exponents are also the same as for the Ising spinodal [56, 57].

To understand the role of the fluctuation structure, we now discuss the significant difference between measurements of the spinodal exponents in Ising models and in supercooled fluids. As can be seen in Fig. 1 and is discussed in Ref. [7], there is no spinodal in an Ising model with a finite-range interaction, but there are pseudospinodal effects if the interaction range is sufficiently long. In particular, as discussed in Sec. IV, we see spinodal-like behavior for $R \gg 1$ as long as the system is not quenched too deeply into the metastable state (see Refs. [7]–[9]). Moreover, the larger the value of R , the more the pseudospinodal behaves like a true spinodal.

In the supercooled liquid there is no direct evidence of a spinodal or pseudospinodal in either experiments or simulations. As we will see, this lack of direct evidence is due to the structure of the fluctuations in mean-field and near-mean-field systems and the crucial role of the fundamental clusters.

For the potential defined in Eq. (146) the system is a fluid for high temperatures and/or low densities as can be seen from the theoretical work in Refs. [56, 57] and in simulations [58]. As we have discussed, if the temperature T is lowered at a fixed density, the liquid-solid spinodal instability is encountered at T_s , the spinodal temperature. If T is lowered below T_s , the uniform density fluid phase is unstable and a “clump” phase is formed. This phase consists of groups or clumps of particles with $\sim R^d$ particles in each clump [58]. These clumps appear to be randomly arranged and the system can be interpreted as a metastable glass. Because we are interested in the signature of the spinodal in this model, the behavior of the system for $T < T_s$ is of no special interest here.

To discuss the role of the fundamental clusters near the spinodal in this model, we first note that, unlike the case for Ising models, there is no precise definition of a cluster in a continuum particle system. However, because we are considering the behavior of the system near a spinodal, we can plausibly argue that the fluctuations and fundamental clusters scale the same as they do near the Ising spinodal. This assumption is given greater weight by the fact that the Ising and spinodal critical exponents for the system defined by the potential in Eq. (146) are the same. For convenience, we will use temperature scaling rather than the analog of magnetic field scaling near the spinodal.

Grewe and Klein treated the mean-field system using the mean-field methodology given by Kac et al. [5]. In particular, the interaction range $R = \gamma^{-1}$ was taken to infinity before the spinodal critical point was approached, that is, before the limit $\Delta\epsilon \propto (T - T_s)$ goes to zero is taken. From Eqs. (136) and (66) the lifetime of the fundamental clusters scales as

$$\tau_{\text{fc},s} \sim \frac{\Delta\epsilon^{-1}}{R^d \Delta\epsilon^{3-d/2}}, \quad (155)$$

as $\Delta\epsilon$ goes to zero. Hence, the Kac limit used by Grewe and Klein treats a system in which there exists fundamental clusters with probability of order one but zero lifetime (see the discussion in Sec. III). That is, the theoretical predictions assume that the limit $R \rightarrow \infty$ is taken before $\Delta\epsilon \rightarrow 0$ and therefore the fundamental cluster lifetime is zero. However, in experiments as well as simulations, the converse is true. For example, consider a measurement of the structure function $S(k)$ in a simulation. The structure function is obtained by computing

$$S(k) = \frac{1}{N} \langle \left[\sum_j e^{i\mathbf{k} \cdot \mathbf{x}_j} \right]^2 \rangle, \quad (156)$$

where \mathbf{x}_j is the (instantaneous) position of the j th particle and $\langle \dots \rangle$ denotes an ensemble average. Because a simulation can only be performed on systems with finite R , the time of the measurement, which is instantaneous, is much shorter than the finite fundamental cluster lifetime in Eq. (155). Therefore the result of the simulations need not be consistent with the theoretical predictions of Grewe and Klein [56, 57]. We stress that the time scale of the measurement does not refer to the time over which data is taken, but the time in which the probe (say a neutron) is in contact with a fluctuation in the system.

Note that in non-mean-field systems only one cluster represents a fluctuation in contrast to fluctuations in mean-field systems which are represented by fluctuations in the number of fundamental clusters (see Sec. VI). Before considering the behavior of the structure function

in supercooled liquids near the spinodal where the measurement is made on a time scale short compared to the lifetime of the fundamental clusters, we discuss the same measurement in the Ising model. We will find that the measured behavior of the structure function in the latter agrees with the theoretically predicted mean-field behavior [37].

Consider the scaling argument for the isothermal susceptibility in Sec. VI. The application of this argument to the susceptibility χ_T near the Ising spinodal gives (see Eqs. (108)–(110))

$$\chi_T \sim \left[\frac{\Delta h^{1/2}}{(R^d \Delta h^{3/2-d/4})^{1/2}} \right]^2 R^d \Delta h^{-d/4} \sim \Delta h^{-1/2}. \quad (157)$$

(The term in brackets is the density of the fluctuations.) We can calculate the isothermal susceptibility using the fundamental clusters as follows. The density of a fundamental cluster is (see Eq. (134))

$$\psi(\mathbf{x}) \sim \frac{\Delta h^{1/2}}{R^d \Delta h^{3/2-d/4}}. \quad (158)$$

The isothermal susceptibility associated with one fundamental cluster is (see Eq. (108)) is

$$\chi_{T, \text{fc}} \sim \left[\frac{\Delta h^{1/2}}{R^d \Delta h^{3/2-d/4}} \right]^2 R^d \Delta h^{-d/4} \sim \frac{\Delta h^{-1/2}}{R^d \Delta h^{3/2-d/4}}. \quad (159)$$

Because the clusters are independent, the total isothermal susceptibility is the sum of the individual cluster isothermal susceptibilities. Because there are $R^d \Delta h^{3/2-d/4}$ clusters (see the discussion in Sec. VI), the isothermal susceptibility is $\Delta h^{-1/2}$ consistent with Eq. (157). Although there are clusters of both up and down spins, each cluster has the same isothermal susceptibility because the susceptibility is proportional to the square of the spin density [33, 34].

Consider another way of obtaining the same result as in Eq. (157). The structure function for one fundamental cluster $S_{\text{fc}}(\mathbf{k})$ is the Fourier transform of the connectedness function of the cluster. We can write (see Eq. (118))

$$S_{\text{fc}, \text{s}}(\mathbf{k}) \sim \left[\frac{\Delta h^{1/2}}{R^d \Delta h^{3/2-d/4}} \right]^2 \delta(\mathbf{k}). \quad (160)$$

The delta function comes from integrating over the assumed infinite size of the spatially uniform cluster. For a cluster with the linear size of the correlation length ξ , the delta function would be replaced by a function whose height is ξ^d and whose width is inversely proportional to ξ .

The fundamental cluster lifetime is (see discussion in Sec. VII)

$$\tau_{\text{fc}, \text{s}} \sim \frac{\Delta h^{-1/2}}{R^d \Delta h^{3/2-d/4}}, \quad (161)$$

in contrast to the lifetime of a fluctuation which is $\sim \Delta h^{-1/2}$. These results suggest the following picture. A fluctuation is a collection of fundamental clusters that appear and disappear on the time scale given in Eq. (161). The lifetime of a fluctuation has a much larger lifetime than a fundamental cluster when the system is near-mean-field, that is, $R^d \Delta h^{3/2-d/4} \gg 1$, which implies that the short lifetime fundamental clusters come and go with different angular orientations but with their centers in roughly the same place for a time of order $\Delta h^{-1/2}$, the lifetime of a fluctuation. If we make a measurement on a time scale large compared to $\Delta h^{-1/2}$, the number of up and down fundamental clusters would be the same on the average and the measured structure function would show no correlation between the spins over this time scale.

We now consider a measurement on a time scale t_{meas} such that $t_{\text{meas}} \gg \tau_{\text{fc,s}}$ and $t_{\text{meas}} \sim \Delta h^{-1/2}$. Because the lifetime of the fluctuations are on the same time scale as the measurement time, the measurement will see a spin density equal to the fluctuation density, which is generated by fluctuations in the number of fundamental clusters. That is, for $t_{\text{meas}} \sim \Delta h^{-1/2}$, the individual fundamental clusters cannot be distinguished, and the structure function will be

$$S(\mathbf{k}) \sim \left[\frac{\Delta h^{1/2}}{(R^d \Delta h^{3/2-d/4})^{1/2}} \right]^2 \delta(\mathbf{k}). \quad (162)$$

If we replace $\delta(\mathbf{k})$ by ξ^d , we obtain the same result as in Eq. (157), obtained by considering the fundamental clusters directly.

Suppose now that the measurement is made on a time scale that is short compared to the lifetime of a fundamental cluster in Eq. (161). The picture now seen by an external probe or by a simulation is a set of order $R^d \Delta h^{3/2-d/4}$ *frozen* fundamental clusters. The structure function of a fundamental cluster is given in Eq. (160). To determine the structure function that would be measured, we need to add the cluster structure function for the $R^d \Delta h^{3/2-d/4}$ frozen clusters. (We ignore numerical factors because we are interested in the scaling properties only.) To add the clusters we convert this sum to an integral by using one of the factors of $1/R^d \Delta h^{3/2-d/4}$ in Eq. (160) to create an infinitesimal element of solid angle $d\Omega$. In so doing we are assuming that on a time scale $t_{\text{meas}} \ll \tau_{\text{fc,s}}$, the $R^d \Delta h^{3/2-d/4}$ fundamental clusters overlap each other with random orientations. Hence the sum over clusters becomes an integral over the solid angle

$$S(|\mathbf{k}|) \sim \int d\Omega \frac{\Delta h}{R^d \Delta h^{3/2-d/4}} \delta(\mathbf{k}). \quad (163)$$

For $d = 3$, we have in spherical polar coordinates

$$S(k) \sim \frac{\Delta h}{R^3 \Delta h^{3/2-3/4}} \int \sin \theta d\theta d\phi \frac{\delta(k)\delta(\theta)\delta(\phi)}{k^2 \sin \theta}, \quad (164)$$

where $k = |\mathbf{k}|$. Hence

$$S(k) \sim \frac{\Delta h}{R^3 \Delta h^{3/2-3/4}} \frac{\delta(k)}{k^2}. \quad (165)$$

If we now replace the delta function $\delta(k)$ by ξ and note that the broadened delta function restricts $k \sim \xi^{-1}$, we obtain

$$S(k) \sim \frac{\Delta h}{R^3 \Delta h^{3/2-3/4}} \xi^3 = \frac{\Delta h}{R^3 \Delta h^{3/2-3/4}} R^3 \Delta h^{-3/4} = \Delta h^{-1/2}, \quad (166)$$

in agreement with Eq. (157). The application of these considerations to arbitrary dimensions is straightforward. We conclude that we obtain the same scaling dependence for the susceptibility (equal to the structure function at $k = 0$), independent of the relative order of magnitude of the measurement time.

We now discuss a measurement of $S(k)$ near the liquid-solid spinodal in supercooled liquids. As before we will assume that the fundamental clusters in the supercooled liquid scale in the same way as they do in Ising models. Because the clusters are independent [40], the structure function of an individual fundamental cluster has to contain information about the symmetry of the approaching instability that is contained in the structure function derived by Grewe and Klein [56, 57] (see (Eq. (149))). That is, a collection of independent clusters cannot generate a symmetry that does not already exist in each individual cluster. Because we are interested in the limit of stability of the supercooled liquid and know that the instability occurs at a wave vector $\mathbf{k}_0 \neq 0$ [56, 57], the clusters must reflect this symmetry. For this reason we will assume that the clusters have a symmetry reflected by a wave vector \mathbf{k}_0 whose magnitude is fixed at the value associated with the instability and whose orientation is arbitrary. In analogy with the Ising spinodal, we expect that the structure function $S_{fc}(\mathbf{k})$ of the fundamental clusters can be approximated near the spinodal by

$$S_{fc,s}(\mathbf{k}) \sim \left[\frac{\epsilon}{R^d \epsilon^{3-d/2}} \right]^2 \delta(\mathbf{k} - \mathbf{k}_0). \quad (167)$$

There may be other structure function peaks at values of $|\mathbf{k}| \neq \mathbf{k}_0$, but we focus on $|\mathbf{k}_0|$ as the largest peak in the structure function of the supercooled liquid and the one associated with the structure function divergence as the spinodal is approached.

We first consider a measurement time scale short compared to the cluster lifetime $\tau_{\text{fc},s}$, which in analogy with the Ising model is

$$\tau_{\text{fc},s} \sim \frac{\epsilon^{-1}}{R^d \epsilon^{3-d/2}}. \quad (168)$$

We have used temperature variables rather than the chemical potential, the analog of the magnetic field. As in the Ising case we need to sum over all orientations of the frozen clusters whose centers are fixed. As before we will convert this sum to an integral by absorbing one of the factors of $1/R^d \epsilon^{3-d/4}$ in Eq. (167) to form an infinitesimal. In this case we need to integrate over orientations of the vector \mathbf{k}_0 keeping the magnitude $|\mathbf{k}_0| = k_0$ constant. The structure function in $d = 3$ becomes

$$S(k) \sim \frac{\epsilon^2}{R^3 \epsilon^{3-3/2}} \frac{1}{k_0^2} \iint d\theta d\phi \delta(k - k_0) \delta(\theta) \delta(\phi). \quad (169)$$

The $\sin \theta$ in the numerator associated with the solid angle in $d = 3$ and the $\sin \theta$ in the denominator associated with the delta function in spherical polar coordinates cancel. The integrals in Eq. (169) give

$$S(k) \sim \frac{\epsilon^2}{R^3 \epsilon^{3-3/2}} \frac{1}{k_0^2} \delta(k - k_0). \quad (170)$$

As in the Ising case the delta function is smeared out when the correlation length ξ is finite. Rather than being infinite at $k = k_0$, its value is the correlation length $\xi \sim R\epsilon^{-1/2}$. Hence, the structure function at $k = k_0$ will scale as

$$S(k_0) \sim \frac{\epsilon^2 R \epsilon^{-1/2}}{R^3 \epsilon^{3-3/2}} = R^{-2} \epsilon^0. \quad (d = 3) \quad (171)$$

Equation (171) implies that in $d = 3$ there is either no divergence or the divergence is logarithmic, which is consistent with the fact that no direct evidence of a pseudospinodal has been observed in simulations of three-dimensional simple fluids such as Lennard-Jones, despite the indirect evidence that nucleation is influenced by a pseudospinodal in deeply quenched Lennard-Jones liquids [16, 59] and in nickel [17].

It is easy to show that $S(k_0)$ for arbitrary dimensions scales as

$$S(k_0) \sim \frac{\epsilon^2 R \epsilon^{-1/2}}{R^d \epsilon^{3-d/2}} = R^{-d+1} \epsilon^{-3/2+d/2} \propto \epsilon^{-\tilde{\gamma}}. \quad (172)$$

In $d = 1$ $S(k) \sim \epsilon^{-1}$, which corresponds to a critical exponent of $\tilde{\gamma} = \gamma = 1$ as predicted by mean-field theory. In $d = 2$, $\tilde{\gamma} = 1/2$ and in $d = 3$, $\tilde{\gamma} = 0$, which differs from the exact result $\gamma = 1$ for all d of Grewe and Klein (see Eq. (149)).

We have performed a test of the prediction in Eq. (172) by measuring the structure function in $d = 1-3$ for the repulsive step potential in Eq. (146) and found results consistent with those predicted [60]. Note that the difference between the spinodal or pseudospinodal in supercooled liquids and the Ising model is that the Ising structure function at the spinodal diverges at $|\mathbf{k}| = 0$, while the supercooled liquid structure function diverges at $|\mathbf{k}_0| = k_0 \neq 0$.

If we were able to do a measurement on a time scale of the order of the fluctuation lifetime ϵ^{-1} , we would see a smeared out density fluctuation that was radially symmetric and varied periodically in the radial direction. We expect that the dominant periodicity would be characterized by the wave vector k_0 and that the divergent contribution to the structure function near the spinodal can be approximated for $k \approx k_0$ by

$$S_{f,s}(k) \sim \frac{\epsilon^2}{R^d \epsilon^{3-d/2}} \int dx x^{d-1} e^{i(k-k_0)x}. \quad (173)$$

Note that we used the density of a fluctuation rather than the cluster, which is appropriate for the time averaged cluster distribution as in the Ising model. At $k = k_0$ the structure function will be given by

$$S_{f,s}(k_0) \sim \frac{\epsilon^2}{R^d \epsilon^{3-d/2}} R^d \epsilon^{-d/2} = \epsilon^{-1}, \quad (174)$$

consistent with the results of Refs. [56, 57].

In summary, the structure and finite lifetime of the fundamental clusters are responsible for the nature of the divergence of the structure function near the liquid-solid spinodal. In Ising models where the peak of the structure function is at $k = 0$, the fact that measurements are made on a time scale short compared to a fundamental cluster lifetime rather than a time scale much longer as required by the theory makes no difference in the measured exponents that characterize the divergence. This result is consistent with the simulations in Ref. [7]. In contrast, when the structure function peak is at a nonzero wave vector, the measurement time scale makes a difference in the observed value of the exponents. These results are consistent with the measurements of the structure function in $d = 3$ Lennard-Jones systems where nucleating droplets consistent with the presence of a spinodal [16, 59] have been found, but no spinodal has been directly observed.

IX. CLUSTER STRUCTURE AND NUCLEATION

The best known theory of nucleation is the classical nucleation theory introduced by Gibbs [19]. In this theory the nucleating droplet is assumed to be isolated, compact, and describable as a fluctuation about a quasi-equilibrium metastable state. Classical nucleation occurs near the coexistence curve independent of the range of interactions in the system [61]. For systems with sufficiently long-range interactions a quench near the pseudospinodal can lead to nucleation being influenced by the critical point nature of the pseudospinodal. Because the spinodal is a critical point, the surface tension will vanish as the spinodal is approached. Near the pseudospinodal the surface tension will not be zero, but nucleation will occur with a very small surface tension [11]. In these circumstances the nucleating droplet is no longer compact as in classical nucleation theory [10, 11]. We will refer to this form of nucleation as *spinodal nucleation*.

There are several ways to approach nucleation theoretically. One of the most elegant was developed most fully by Langer [18, 19] and adapted to spinodal nucleation by Klein and Unger [11, 62]. In this approach the Landau-Ginzburg-Wilson Hamiltonian (see Eq. (4))

$$\beta H(\phi) = \beta \int d\mathbf{x} \left[\frac{R^2}{2} (\nabla \phi(\mathbf{k}))^2 + \epsilon \phi^2(\mathbf{x}) + \phi^4(\mathbf{x}) - h \phi(\mathbf{x}) \right] \quad (175)$$

is used to calculate the free energy $F(\beta, h)$ in the equilibrium state

$$F(\beta, h) = -k_B T \ln \int \delta \phi e^{-\beta H(\phi)}, \quad (176)$$

which can then be analytically continued from the stable to the metastable state [18]. Langer [18] associates the nucleating droplet with the solution to the Euler-Lagrange equation obtained from the functional derivative of the Landau-Ginzburg-Wilson Hamiltonian.

$$-R^2 \nabla^2 \phi(\mathbf{x}) - 2|\epsilon| \phi(\mathbf{x}) + 4\phi^3(\mathbf{x}) - h = 0. \quad (177)$$

In Eq. (177) ϵ is taken to be less than zero, that is, the temperature T is below the critical temperature. The dominant exponential part of the nucleation probability is obtained by substituting the solution to Eq. (177) into the expression for the imaginary part of the analytically continued free energy. The details of this approach can be found in Langer's original paper [18] and is outlined in Ref. [19].

Klein and Unger expanded the Landau-Ginzburg-Wilson Hamiltonian about the mean-field spinodal ϕ_s by defining a new field $\phi(\mathbf{x}) - \phi_s$, where ϕ_s is the order parameter density

at the spinodal [62]. They obtained an Euler-Lagrange equation of the form

$$-R^2 \nabla^2 \psi(\mathbf{x}) + \lambda_1 \Delta h^{1/2} \psi(\mathbf{x}) - \lambda_2 \psi^2(\mathbf{x}) = 0 \quad (178)$$

after performing a shift accomplished by defining $\psi(\mathbf{x}) = \phi(\mathbf{x}) - \phi_s + a$; a is a constant that is fixed by the condition that the term linear in $\psi(\mathbf{x})$ does not appear in the Landau-Ginzburg-Wilson Hamiltonian. In Eq. (178) λ_1 and λ_2 are constants for fixed ϵ , $\Delta h = h_s - h$, and h_s is the spinodal value of the field for the assumed value of ϵ .

It is straightforward to show that the solution to Eq. (178) must have the scaled form [11, 62]

$$\psi(\mathbf{x}) = \Delta h^{1/2} f\left(\frac{\mathbf{x}}{R \Delta h^{-1/4}}\right), \quad (179)$$

which implies that the difference in the order parameter density between the interior of the droplet and the metastable state background is the order of $\Delta h^{1/2}$. This scaling implies that this difference is vanishingly small for large R and small Δh . This vanishingly small order parameter difference presents two problems: how can we identify when and where the nucleating droplet occurs and how can we determine the structure of the droplet. In Ising models these problems have been solved by the mapping of the spinodal onto a percolation transition and investigating the relation between the clusters and the nucleating droplet.

As we have found, the density of the nucleating droplet over the background metastable state is of the order of $\Delta h^{1/2}$ (Eq. (179)), the density of the fundamental clusters is $\Delta h^{1/2}/R^d \Delta h^{3/2-d/4}$ (Eq. (134)), and the density of a fluctuation is $\Delta h^{1/2}/(R^d \Delta h^{3/2-d/4})^{1/2}$ (see the discussion in Sec. IV). Clearly, the nucleating droplet is not a fundamental cluster or a fluctuation described by the Gaussian approximation. From the discussion in Sec. VII we have that the fluctuations near a spinodal are generated by random walks of the number of fundamental clusters in the up or down direction. A possible scenario might be that the nucleating droplet is generated by a random walk in the number of fundamental clusters that produces a region of density $\Delta h^{1/2}$. From the discussion in Secs. VI and VII such a process would require a “walk” of distance $R^d \Delta h^{3/2-d/4}$ ($[R^d \Delta h^{3/2-d/4}]^2$ steps) and a time of $\tau \sim \Delta h^{-1/2} R^d \Delta h^{3/2-d/4}$. Because the nucleation time is the inverse of the probability (see Ref. [18]), the nucleation time would be of the order of $\exp(\beta R^d \Delta h^{3/2-d/4})$. We conclude that a random walk occurs too quickly to account for the time needed to see nucleation.

A clue to the relation between the fundamental clusters and the nucleating droplets is provided by Monette and Klein [12] who simulated a two-dimensional Ising model with long-

range interactions. Nucleation was observed near the spinodal and the nucleating droplet was identified using an intervention technique [12]. They found that the number of fundamental clusters just prior to nucleation was on the order of $G_s = R^d \Delta h^{3/2-d/4} = R^2 \Delta h \gg 1$ ($d = 2$), implying that the G_s fundamental clusters with density $\Delta h^{1/2}/G_s^{1/2}$ coalesced into an object or cluster with a density on the order of $\Delta h^{1/2}$.

The results of Monette and Klein together with the random walk argument suggests the following picture of the relation between the fundamental clusters and the nucleating droplets. While the system is in the metastable state, there are fluctuations in the number of fundamental clusters. These fluctuations result in regions with order $R^d \Delta h^{3/2-d/4}$ fundamental clusters in excess of the background on a time scale $\sim R^d \Delta h^{3/2-d/4} \Delta h^{-1/2}$. Because this time scale is small compared to the time scale for nucleation, which is of the order of $\exp[\beta R^d \Delta h^{3/2-d/4}]$ [11], the appearance of $R^d \Delta h^{3/2-d/4}$ clusters with a linear spatial extent of the correlation length will happen everywhere in the system many times before the nucleation event. In Fig. 3 we plot the number of fundamental clusters the size of the correlation length in a region where we know that nucleation will occur. Notice the number of time intervals where the number of fundamental clusters is of order $R^d \Delta h^{3/2-d/4}$.

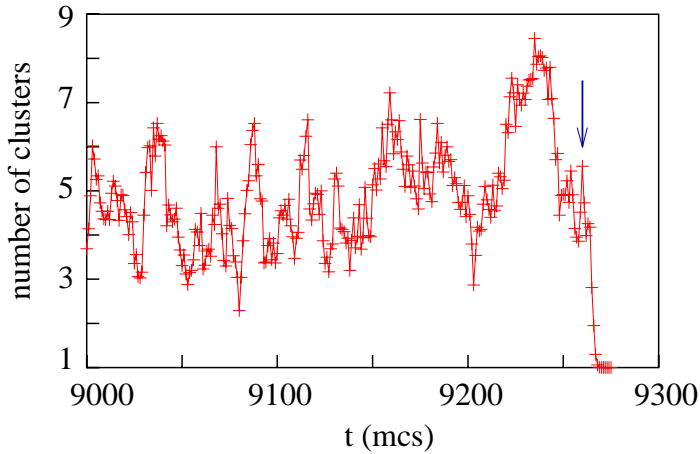


FIG. 3: The number of clusters in a region the size of the correlation length where nucleation will occur (see arrow). Note the number of times where the number of fundamental clusters is of order G_s . The Monte Carlo simulation was done for a two-dimensional Ising model with $R = 28$, $h = 1.25$, $G_s = 12.3$, and linear dimension $L = 560$.

Because the time scale for nucleation is of the order of $\exp[\beta R^d \Delta h^{3/2-d/4}]$ and the $R^d \Delta h^{3/2-d/4}$ fundamental clusters coalesce at nucleation, we must assume that there is a

free energy cost associated with the coalescence that is of the order of $R^d \Delta h^{3/2-d/4}$. We can estimate this free energy cost by noting that the coalescence of the $R^d \Delta h^{3/2-d/4}$ fundamental clusters does not change the density by more than an infinitesimal amount. This assumption is justified because the random walk is assumed to generate a density in the stable phase direction of order $\Delta h^{1/2}$ and the nucleating droplet has the same density. Therefore the energy change due to coalescence is negligible. The entropy cost can be estimated by noting that there are $R^d \Delta h^{3/2-d/4}$ fundamental clusters before nucleation and one cluster which is the nucleating droplet after coalescence. These considerations imply that the entropy change is given by

$$\Delta S \sim \ln 2 - \ln 2^{R^d \Delta h^{3/2-d/4}} \sim R^d \Delta h^{3/2-d/4} \ln 2, \quad (180)$$

because each cluster has two states, up and down. Since the energy change is negligible, the free energy change due to coalescence is on the order of $R^d \Delta h^{3/2-d/4} \gg 1$. Because the probability of nucleation is $\propto e^{-\beta \Delta F}$, the probability of coalescence and hence nucleation is $\sim \exp[-\beta R^d \Delta h^{3/2-d/4}]$ in agreement with the calculation in Refs. [11, 62].

This discussion and the one in Sec. VIII suggests that the fundamental clusters are not just a mathematical construct. They appear to carry information on a level not described by the standard approaches of statistical mechanics and are real physical objects. This suggestion will be given further credence by the discussion in the next section.

X. CLUSTERS AND MODELS OF EARTHQUAKE FAULTS

In this section we will discuss the relevance of the cluster structure to our understanding of earthquakes. To do so we will discuss several models that have received much recent attention. The first is the Burridge-Knopoff model introduced in 1967 [63]. The original model consists of blocks connected by linear springs to their nearest neighbors with spring constant k_c . The blocks are also connected to a loader plate by linear springs with spring constant k_L , and rest on a surface with a nonlinear velocity-weakening stick-slip friction force.

The simulation is initiated by choosing the displacements of the blocks at random. While the loader plate is fixed, we determine the stress on each block and update its velocity and displacement according to Newton's equations of motion. We continue this process until all blocks are stuck. A block is considered to be “stuck” when its velocity is below a certain

threshold and other criterion are met (see Refs. [64–66] for details). We then add stress to all the blocks by moving the loader plate to bring the block with the largest stress to failure. That is, when the stress on a block exceeds the static coefficient of friction, the block “fails” and the block begins to slip. This process insures that there will be only one block that initiates the failure sequence. An earthquake is comprised of all the blocks that fail between plate updates.

The number n_s of earthquakes with s blocks exhibits a power law dependence on s . That is,

$$n_s \sim s^{-x}, \quad (181)$$

with $x \approx 2$ if the springs are connected by only nearest-neighbor blocks [64–66]. However, the calculation of realistic stress transfer Green’s functions for real faults [67, 68] indicates that we should include springs that connect further neighbor blocks. The behavior of the Burridge-Knopoff model is more complicated in this case and in the limit of long-range stress transfer and a slow decrease of the velocity-weakening friction force with increasing velocity, it has been found in simulations that $x \approx 3/2$ [66].

To provide more insight into the behavior of the model with long-range springs we will discuss a cellular automaton (CA) version of the Burridge-Knopoff model introduced by Rundle, Jackson, and Brown [69–71]. We consider the same blocks and springs as in the Burridge-Knopoff model, but instead of including a friction force between the blocks and the substrate, we define a set of rules for the displacement of each block and the stress on it. We first specify a failure threshold σ_F and a residual stress σ_R for each block. For simplicity, we will take the σ_F and σ_R to be the same for all blocks. The stress on a block is given by $\sigma_j = k_L(\Delta - u_j) + k_c \sum_i (u_i - u_j)$, where Δ is the displacement of the loader plate and u_j is the displacement of block j from its initial position. The blocks are checked to see if any have a stress $\sigma_j \geq \sigma_F$. If $\sigma_j < \sigma_F$, we do nothing and proceed to the next block. If $\sigma_j \geq \sigma_F$, we move the block a distance Δu where

$$\Delta u_j = \frac{\sigma_j - \sigma_R}{k_L + qk_c}, \quad (182)$$

where q is the number of neighbors of the j th block. If the lattice is a square array with only nearest-neighbor blocks connected by springs, then $q = 4$. If the range of stress transfer is R , then $q = (2R + 1)^2$. Once the system is quiescent, that is, $\sigma_j < \sigma_F$ for all j , the plate

is updated as described for the Burridge-Knopoff model. An earthquake is the set of blocks that fail between plate updates.

As in the Burridge-Knopoff model, the number of earthquakes with s failed blocks has a power law dependence as in Eq. (181). In the long-range CA model $x = 3/2$. How does this scaling arise? Is it associated with critical point behavior? A clue is given by the fact that the long-range stress transfer CA models with noise added to the stress drop can be described by equilibrium statistical mechanics [72, 73]. In addition, it has been shown that this model can be described by a Langevin or Landau-Ginzburg equation in the limit $R \rightarrow \infty$ [74]. The latter equation has the same form as Eq. (101) (see Ref. [3]). These considerations imply that the scaling behavior $n_s \sim s^{-3/2}$ in the long-range CA models is due to a spinodal similar to what has been found in Ising models with long-range interactions.

To obtain the scaling exponent x for the long-range earthquake CA models, we use the fact that the Ising critical point can be described by a Fisher droplet model [75]. In this model the system near a critical point can be described by a collection of non-interacting or independent droplets. The distribution of the droplets is given by

$$\tilde{n}_s \sim \frac{e^{-\Delta h s^{\tilde{\sigma}}}}{s^{\tau}}. \quad (183)$$

It should be clear from the cluster mapping near the spinodal discussed in Sec. V that the Fisher droplets are the usual Ising clusters near the spinodal. To obtain the exponent τ , which is related to the exponent x in Eq. (181), we note that the Fisher droplet model exponents are related to the spinodal exponents derived in Sec. IV through the first several moments of Eq. (183). In particular, the isothermal susceptibility χ_T is given by the second moment of \tilde{n}_s

$$\chi_T \propto \int ds s^2 \frac{e^{-\Delta h s^{\tilde{\sigma}}}}{s^{\tau}} \propto \Delta h^{-1/2}, \quad (184)$$

and the order parameter density ψ (see Sec. V) is related to the first moment of \tilde{n}_s

$$\psi \propto \int ds s \frac{e^{-\Delta h s^{\tilde{\sigma}}}}{s^{\tau}} \propto \Delta h^{1/2}. \quad (185)$$

Here we have kept G_s constant and used the fact that hyperscaling holds and the density of the fluctuations scales as $\Delta h^{1/2}$. (see Eq. (56c)). This constraint is the appropriate one for the earthquake fault models we are considering because these models self-organize to run at a distance from the spinodal (the variable analogous to Δh), where $G_s \sim 3-5$. A more

complete discussion of this point is given in Ref. 3. We can assume that the exponential in the integrals is approximately one until $s^{\tilde{\sigma}} \sim \Delta h^{-1}$. Hence,

$$\frac{3 - \tau}{\tilde{\sigma}} = \frac{1}{2}, \quad (186)$$

and

$$\frac{\tau - 2}{\tilde{\sigma}} = \frac{1}{2}. \quad (187)$$

Equations (186) and (187) yield $\tau = 5/2$ which does not apparently agree with the measured value of $x = 3/2$. However, the exponents obtained by this reasoning assume that the cluster distribution is obtained by tossing bonds between occupied sites as explained in Sec. IV. In the earthquake case the clusters are grown from a seed, that is, the initiator site, which is brought to failure by a loader plate update. For clusters grown from a seed the counting is slightly different [42]. Because for a cluster of size s there are s places that could have been the seed, the number of such clusters is sn_s , where n_s is given in Eq. (181). Hence, the prediction is that $\tau = x + 1$ and hence $x = 3/2$, in agreement with the simulations of models with long-range stress transfer. However, the scaling form for n_s with $x \approx 2$ for the usual Burridge-Knopoff model with short-range interactions is not understood.

There are other properties of the distribution of earthquakes in the Rundle-Jackson-Brown CA model that can be obtained from consideration of the clusters in Ising models near spinodals. We refer the interested reader to Ref. [3]. The relation between the CA and Burridge-Knopoff models for long-range stress transfer can be found in Refs. [76, 77].

XI. SUMMARY AND CONCLUSIONS

We have obtained information about the structure of the clusters at mean-field critical points and spinodals in Ising models and simple fluids. The cluster structure and its relation to the structure of thermal fluctuations is more complicated in mean-field and near-mean-field systems than the corresponding relation in systems that are not mean-field and which obey hyperscaling. For mean-field and near-mean-field systems the thermal fluctuations are generated by fluctuations in the number of fundamental clusters. Because the clusters in mean-field and near-mean-field systems play a different role and appear to be real physical objects rather than just mathematical constructs, we refer to them as fundamental clusters. Their physical consequences was seen most clearly in Sec. VIII in the discussion on spin-

odals in supercooled liquids. In this case the relation between the measurement time and the lifetime of the fundamental clusters gives rise to predictions about structure function measurements that are contrary to rigorous mean-field theory and are yet confirmed by the simulations on near-mean-field systems. We emphasize that the probability of finding a fundamental cluster is not given by the Boltzmann factor because its lifetime is much less than the decorrelation time (see the discussion at the end of Sec. III).

In addition to the three applications of the cluster structure discussed in this paper, there are many other applications that have shed light on physical processes. These applications include:

1. The elucidation of the early time structure of systems undergoing spinodal decomposition and continuous ordering, including the understanding of why the linear theory of Cahn, Hilliard, and Cook [20–22] fails first at large momentum transfer [23, 24]), the fractal structure of the mass distribution of early time spinodal decomposition [25], and a physical interpretation of the fermionic (Grassman) variables associated with a supersymmetric representation of the early stage continuous ordering [23, 24, 78].
2. The phase separation of polymer and solvent in the presence of gelation [79].
3. Possible precursors to nucleation near the pseudospinodal [12].

Future work includes the application of cluster methods to the study of precursors to large earthquakes in the CA and Burridge-Knopoff models, the study of heterogeneous nucleation near pseudospinodals, the investigation of fracture and the merging of microcracks, and the study of the crossover from the linear regime of spinodal decomposition and continuous ordering to the nonlinear evolution.

Acknowledgments

We are pleased to acknowledge useful conversations with F. Alexander, M. Anghel, G. G. Batrouni, A. Coniglio, C. Ferguson, G. Johnson, L. Monette, T. Ray, and P. Tamayo. W. Klein and J. B. Rundle received support from the DOE grant #s DE-FG02-95ER14498 and DE-FG03-95ER14499, respectively, K. F. Tiampo was supported by an NSERC Discovery Grant, and H. Gould and N. Gulbahce were supported in part by NSF DUE-0127363. This

work was partly carried out under the auspices of the National Nuclear Security Administration of the U.S. Department of Energy at Los Alamos National Laboratory under Contract No. W-7405-ENG-36.

- [1] S. R. Shenoy, T. Lookman, A. Saxena, and A. R. Bishop, Phys. Rev. B **60**, R12537 (1999).
- [2] W. Klein, T. Lookman, A. Saxena, and D. Hatch, Phys. Rev. Lett. **88**, 085701 (2002).
- [3] W. Klein, M. Anghel, C. D. Ferguson, J. B. Rundle, and J. S. Sá Martins, in *GeoComplexity and the Physics of Earthquakes*, edited by J. B. Rundle, D. L. Turcotte and W. Klein (American Geophysical Union, Washington, DC, 2000).
- [4] K. Binder, Phys. Rev. A **29**, 341 (1984).
- [5] M. Kac, G. E. Uhlenbeck, and P. Hemmer, J. Math. Phys. **4**, 216 (1963).
- [6] The systems we consider in this paper have standard thermodynamic and statistical mechanical descriptions unlike the systems studied by Tsallis and collaborators. See for example, C. Tsallis in *Lecture Notes in Physics* (Springer, Berlin, 2001).
- [7] D. W. Heermann, W. Klein, and D. Stauffer, Phys. Rev. Lett. **49**, 1262 (1982).
- [8] M. Novotny, W. Klein, and P. Rikvold, Phys. Rev. B **33**, 7729 (1986).
- [9] N. Gulbahce, H. Gould, and W. Klein, Phys. Rev. E **69**, 036119 (2004).
- [10] D. W. Heermann and W. Klein, Phys. Rev. Lett. **50**, 1062 (1983).
- [11] C. Unger and W. Klein, Phys. Rev. B **29**, 2698 (1984).
- [12] L. Monette and W. Klein, Phys. Rev. Lett. **68**, 2336 (1992).
- [13] W. Klein and F. Leyvraz, Phys. Rev. Lett. **57**, 2485 (1986).
- [14] W. Klein, Phys. Rev. E **64**, 056110 (2001).
- [15] J. Yang, H. Gould and W. Klein, Phys. Rev. Lett. **60**, 2665 (1988).
- [16] J. Yang, H. Gould, W. Klein, and R. Mountain, J. Chem. Phys. **93**, 711 (1990).
- [17] F. J. Cherne, M. I. Baskes, R. B. Schwarz, S. G. Srinivasan, and W. Klein, Modelling Simul. Mater. Sci. Eng. **12**, 1063 (2004).
- [18] J. S. Langer, Ann. Phys. (NY) **41**, 108 (1967).
- [19] J. Gunton, P. Sahni, and M. S. Miguel in *Phase Transitions and Critical Phenomena*, edited by C. Domb and J. Lebowitz (Academic Press, NY, 1983), Vol. 8.
- [20] J. W. Cahn, Trans. Metall. Soc. AIME **242**, 166 (1968).

- [21] J. E. Hilliard, in *Phase Transformations*, edited by H. I. Aronson (American Society for Metals, Metals Park, OH, 1970).
- [22] H. E. Cook, *Acta Metall.* **18**, 297 (1970).
- [23] N. Gross, W. Klein, and K. Ludwig, *Phys. Rev. Lett.* **73**, 2639 (1994).
- [24] N. Gross, W. Klein, and K. Ludwig, *Phys. Rev. E* **56**, 5160 (1997).
- [25] W. Klein, *Phys. Rev. Lett.* **65** 1462 (1990).
- [26] J. B. Rundle, W. Klein, S. Gross, and D. L. Turcotte, *Phys. Rev. Lett.* **75**, 1658 (1995).
- [27] C. Ferguson, W. Klein, and J. B. Rundle, *Phys. Rev. E* **60**, 1374 (1999).
- [28] J. B. Rundle, E. Preston, S. McGinnis, and W. Klein, *Phys. Rev. Lett.* **80**, 5698 (1998).
- [29] L. D. Landau and E. M. Lifshitz, *Statistical Physics* (Pergamon Press, Oxford, 1980).
- [30] G. Parisi and N. Sourlas, *Phys. Rev. Lett.* **43**, 744 (1979).
- [31] N. Sourlas, in *Supersymmetry in Physics*, edited by V. A. Kostelecky and D. K. Campbell (North-Holland, Amsterdam, 1985).
- [32] D. Amit, *Field Theory, the Renormalization Group and Critical Phenomena* (World Scientific, Singapore, 2005).
- [33] S. K. Ma, *Modern Theory of Critical Phenomena* (Benjamin, Reading, MA, 1976).
- [34] H. E. Stanley, *Introduction to Phase Transitions and Critical Phenomena* (Oxford University Press, Oxford, 1971).
- [35] P. C. Hohenberg and B. I. Halperin, *Rev. Mod. Phys.* **49**, 435 (1977).
- [36] H. Gould, J. Tobochnik, and W. Christian *An Introduction to Computer Simulation Methods* (Addison Wesley, San Francisco, 2006).
- [37] C. Domb and H. W. Dalton, *Proc. Phys. Soc. London* **89**, 859 (1966).
- [38] C. N. Yang and T. D. Lee, *Phys. Rev.* **87**, 404 (1952).
- [39] T. D. Lee and C. N. Yang, *Phys. Rev.* **87**, 410 (1952).
- [40] A. Coniglio and W. Klein, *J. Phys. A* **13**, 2775 (1980).
- [41] P. Kastaleyn and C. M. Fortuin, *J. Phys. Soc. Jpn. (suppl)* **26**, 11 (1969).
- [42] D. Stauffer and A. Aharony, *Introduction to Percolation Theory* (Taylor and Francis, London, 1992) and references therein.
- [43] K. K. Murata, *J. Phys. A* **11**, L199 (1979).
- [44] K. Huang, *Statistical Mechanics* (Wiley, New York, 1988).
- [45] G. E. Uhlenbeck and G. W. Ford, *Lectures in Statistical Mechanics* (American Mathematical

Society, Providence, RI, 1963).

[46] N. Goldenfeld, *Lectures on Phase Transitions and the Renormalization Group* (Perseus Books, Reading, MA, 1992).

[47] A. Coniglio and T. Lubensky, *J. Phys. A* **13**, 1732 (1980).

[48] T. Ray and W. Klein, *J. Stat. Phys.* **61**, 891 (1990).

[49] We assume that $\rho^{(2)}2(\mathbf{x})$ is a constant for $|\mathbf{x}| < \xi$ and $\rho \sim \epsilon^\beta$.

[50] P. Tamayo, R. Brower, and W. Klein, *J. Stat. Phys.* **58**, 1083 (1990).

[51] W. Klein et al., in preparation.

[52] G. Andronico, A. Coniglio, and S. Fortunato, *Nucl. Phys. Proc. Suppl.* **119**, 876–878 (2003), hep-lat/0208009.

[53] J. G. Kirkwood, in *Phase Transitions in Solids*, edited by R. Smoluchowski, J. E. Mayer, and A. Weyl (Wiley, New York, 1951).

[54] T. L. Hill, *Statistical Mechanics, Principles and Selected Applications* (Dover, New York, 1956).

[55] R. Lovett, *J. Chem. Phys.* **66**, 1225 (1977) and references therein.

[56] N. Grewe and W. Klein, *J. Math. Phys.* **18**, 1729 (1977).

[57] N. Grewe and W. Klein, *J. Math. Phys.* **18**, 1735 (1977).

[58] A. Mel'cuk, R. Ramos, H. Gould, W. Klein, and R. Mountain, *Phys. Rev. Lett.* **75**, 2522 (1995).

[59] P. R. ten Wolde, M. J. Ruiz-Montero, and D. Frenkel, *J. Chem. Phys.* **104**, 9932 (1996).

[60] W. Klein, H. Gould, J. Tobochnik, F. J. Alexander, M. Anghel, and G. Johnson, *Phys. Rev. Lett.* **85**, 1270 (2000).

[61] C. Unger and W. Klein, *Phys. Rev. B* **31**, 6127 (1985).

[62] W. Klein and C. Unger, *Phys. Rev. B* **28**, 445 (1983).

[63] R. Burridge and L. Knopoff, *Bull. Seismol. Soc. Am.* **57**, 341 (1967).

[64] J. M. Carlson and J. S. Langer, *Phys. Rev. A* **40**, 6470 (1989).

[65] J. M. Carlson, J. S. Langer, B. E. Shaw, and C. Tang, *Phys. Rev. A* **44**, 884 (1991).

[66] J. Xia, H. Gould, W. Klein, and J. B. Rundle, *Phys. Rev. Lett.* **95**, 248501 (2005).

[67] J. A. Steketee, *Can. J. Phys.* **36**, 192 (1958).

[68] K. Rybicki in *Continuum Theories in Solid Earth Physics*, edited by R. Teisseyre (Elsevier, Amsterdam, 1986).

- [69] J. B. Rundle and D. D. Jackson, Bull. Seismol. Soc. Am. **67**, 1363 (1977).
- [70] J. B. Rundle and S. R. Brown, J. Stat. Phys. **65**, 403 (1991).
- [71] The model introduced independently by Z. Olami, H. J. S. Feder, and K. Christensen, Phys. Rev. Lett. **68**, 1244–1247 (1992) is identical to the Rundle-Jackson-Brown model if only stress is considered.
- [72] J. B. Rundle, W. Klein, S. Gross, and D. L. Turcotte, Phys. Rev. Lett. **75**, 1658 (1995).
- [73] C. D. Ferguson, W. Klein, and J. B. Rundle, Phys. Rev. E **60**, 1374 (1999).
- [74] W. Klein, J. B. Rundle, and C. D. Ferguson, Phys. Rev. Lett. **78**, 3793 (1997).
- [75] M. E. Fisher, Physics **3**, 255 (1967).
- [76] J. Xia, H. Gould, W. Klein, and J. B. Rundle, Phys. Rev. Lett. **95**, 248501 (2005).
- [77] J. Xia, H. Gould, W. Klein, and J. B. Rundle, cond-mat 0601679.
- [78] W. Klein and G. G. Batrouni, Phys. Rev. Lett. **67**, 1278 (1991).
- [79] A. Coniglio, H. E. Stanley, and W. Klein, Phys. Rev. B **25**, 6805 (1982).